Physics – Uspekhi **50** (9) 907 – 931 (2007)

REVIEWS OF TOPICAL PROBLEMS PACS numbers: **36.40. – c**, 52.40.Hf, 52.40.Mj, **61.46. – w**

Femtosecond excitation of cluster beams

V P Krainov, B M Smirnov, M B Smirnov

DOI: 10.1070/PU2007v050n09ABEH006287

Contents

Abstract. Fast processes of cluster excitation under the action of an ultrashort superpower laser pulse or as a result of cluster collisions are considered. Processes are studied for cluster absorption of a laser pulse and the subsequent evolution of a forming cluster plasma, as well as the evolution of a cluster plasma initiated by cluster collisions. The properties of this plasma as a source of X-ray emission are analyzed. The generation of neutrons results from the excitation of a deuterium cluster beam by a laser pulse and from the collision of an accelerated beam of deuterium clusters with a deuterium target, including a dense beam of deuterium clusters.

1. Introduction

According to their nature, cluster beams are intermediate in composition between solid and gaseous targets. Cluster beams consist of groups of free clusters and each cluster contains from several thousand up to several million atoms and has a size up to several dozen nanometers. On the one hand, the action of high-energy sources on clusters allows reaching a high degree of matter excitation because clusters have a relatively small mass, and, on the other hand, a solid density of atoms in clusters provides a high efficiency of their excitation compared to gaseous systems.

A strong excitation transforms clusters to a fully ionized plasma which is located first in a region occupied by clusters and then freely expands into the surrounding space. For efficient excitation of clusters it is necessary that the time of energy input be small compared to the time of plasma expansion. The expansion time reaches $10^{-13}-10^{-12}$ s for a typical cluster size of 10 nm ($\sim 10^4$ atoms per cluster) and ion flying-apart velocity of 10^7-10^8 cm s^{-1}. This requires femtosecond times for plasma creation and cluster excitation.

We will consider below two methods of femtosecond cluster excitation as a result of excitation of a cluster beam by a femtosecond laser pulse and in collisions of two cluster beams. In the first case, the laser pulse energy is transformed to the energy of cluster excitation, and in the second case the cluster excitation energy is taken from the kinetic energy of cluster beams. Since collective effects are not significant for the transformation of the kinetic energy of not too large clusters into the excitation energy, the character of this process is analogous to the character of the passage of fast ions through clusters. Then, excitation is determined by the passage of individual fast ions through a cluster, and chemical bonds between cluster atoms are not essential to the character of this excitation.

At the first stage of excitation, a nonuniform plasma is formed, being consisted of electrons and multiply charged ions located in the regions where the clusters were found initially. A subsequent decay of a plasma as a result of expansion of such regions leads to essential deceleration of plasma excitation and smearing of nonuniformities. In the

V P Krainov Moscow Institute of Physics and Technology (State University), Institutskii per. 9, 141700 Dolgoprudnyi, Moscow region, Russian Federation
E-mail: krainov@online.ru
B M Smirnov Joint Institute for High Temperatures, Russian Academy of Sciences, ul. Izhorskaya 13/19, 127412 Moscow, Russian Federation
Tel./Fax (7-499) 190 42 44
M B Smirnov Russian Research Centre 'Kurchatov Institute', pl. Kurchatova 1, 123182 Moscow, Russian Federation
E-mail: smirnov@imp.kiae.ru

Received 1 November 2006, revised 26 February 2007
Uspekhi Fizicheskikh Nauk **177** (9) 953 – 981 (2007)
Translated by B M Smirnov; edited by A Radzig

end, a uniform plasma is formed in the total region that was occupied by clusters from the beginning. Therefore, plasma excitation ceases due to a sharp decrease in the density but the energy absorbed by plasma is still retained in it.

Two methods of application of the forming plasma will be considered: as a source of X-ray radiation, and a neutron generator. The process of the formation and evolution of a plasma under the action of an ultrashort high-power laser pulse is accompanied by X-ray emission of this laser-excited cluster plasma [1–7], and the efficiency of laser energy transformation to the energy of X-ray radiation can reach 10% [8, 9]. The creation of efficient X-ray sources is analogous to the creation of excimer lasers in the 1970s, which was a result of the development of nanosecond technique. Then, the efficiency of transformation of nanosecond pulse energy into the energy of ultraviolet radiation also reached 10%. Developing a new time range for sources of electromagnetic energy is now leading to the creation of new sources of electromagnetic energy in a new wavelength range. The main focus in this review will be the general concepts framed for describing plasma processes and a contemporary understanding of this problem.

The energy deposited to the cluster plasma under the action of a femtosecond laser pulse or as a result of collisions of two fast cluster beams is transformed into the energy of X-ray radiation or leads to neutron production in the course of the total time of the plasma's existence. These processes are determined by the properties of this plasma and the character of its evolution. The totality of these problems, which in the case of laser excitation of cluster plasma were considered in reviews [10–13], is the subject of this article.

2. Laser irradiation of cluster beams

2.1 Interaction of femtosecond high-power laser pulses with atomic matter

Creating laser generators of ultrashort superintense pulses of electromagnetic energy transfers the problem of interaction between radiation and atomic matter into new positions. Indeed, a characteristic atomic value for the electric field strength, constructed on the basis of atomic units, is estimated as

$$F_0 = \frac{e}{a_0^2} = \frac{m_e^2 e^5}{\hbar^4} = 5.14 \times 10^9 \text{ V cm}^{-1}, \tag{2.1}$$

and the following intensity of an electromagnetic wave corresponds to this electric field strength:

$$I = \frac{cF_0^2}{8\pi} = 3.5 \times 10^{16} \text{ W cm}^{-2}. \tag{2.2}$$

Here, e is the electron charge, a_0 is the Bohr radius, m_e is the electron mass, $\hbar$ is the Planck constant, and c is the speed of light. The parameters of laser pulses in a contemporary setup exceed the above value by several orders of magnitude. Table 1 lists the parameters of laser pulses for some contemporary setups. As is seen, the intensities of laser pulses emitted by these setups significantly exceed the atomic intensity (τ is the pulse duration, P is the maximum signal power, and I is the maximum intensity of a focussed laser pulse). Of course, each setup generating short superintense laser pulses is unique. The fact that laboratory generation of electric fields exceeds atomic ones was difficult to foresee early, and the existence of a line of such setups raises the reliability of investigations conducted on the basis of these setups.

Table 1. Parameters of short power laser pulses emitted by indicated setup up to 2006.

No.	Institution (country)	τ, fs	P, 10^{12} W	I, W cm^{-2}
1	Univ. of Michigan (USA)	30	40	2×10^{19}
2	Lund (Sweden)	30	30	1×10^{19}
3	LOA (France)	30	100	5×10^{19}
4	Univ. of California (San Diego, USA)	30	50	5×10^{19}
5	MBI (Berlin, Germany)	30	100	1×10^{19}
6	Astra (Great Britain)	40	40	3×10^{18}
7	APRC (JAERI, Japan)	30	500	1×10^{20}
8	ATLAS (Germany)	100	30	5×10^{18}
9	Univ. of Texas (USA)	35	20	2×10^{17}
10	LULI (France)	30	100	5×10^{19}

We are guided in this paper by the intensities I of laser radiation ranging from 10^{16} to 10^{19} W cm^{-2}, which corresponds to the maximum electric field strength $F = (0.6-20)F_0$ of an electromagnetic wave. The duration of electromagnetic field pulses for a real laser setup is 30–100 fs, corresponding to 15–50 periods of oscillations of the electromagnetic wave. In addition, the electromagnetic field frequency is small compared to a typical atomic value.

In considering the interaction between an electromagnetic wave and atomic matter, we will rely on the following peculiarities of this interaction in reality. First, the pulse power is very high, so that its action remarkably changes the behavior of bound electrons. Second, the electromagnetic wave frequency ω is small compared to an atomic one, namely

$$\omega \ll \omega_0 = \frac{m_e e^4}{\hbar^3}, \tag{2.3}$$

and the wavelength corresponding to the atomic frequency ω_0 is equal to

$$\lambda_0 = \frac{2\pi c}{\omega_0} = 2\pi a_0 \frac{\hbar^2}{ce^2} = 45.5 \text{ nm}. \tag{2.4}$$

In particular, in the case of the resonant radiative transition in a sodium atom with a wavelength of $\lambda = 0.6$ μm, the appropriate wavelength ratio λ/λ_0 equals approximately 1/13, and in the case of a titanium–sapphire laser with $\lambda = 0.78$ μm that is usually used as a source of femtosecond laser pulses, this ratio reaches 1/17.

Being guided by such wavelengths and high strengths of the electromagnetic field compared to atomic ones, we arrive at the fact that the Keldysh parameter, which determines the character of interaction between an electromagnetic wave and an atomic system, is small. This is valid both for atoms and for ions resulting from successive ionization of atoms and ions in clusters. Indeed, the Keldysh parameter is defined as [14]

$$\gamma = \frac{\omega}{\omega_0} \frac{F_0}{F} \sqrt{\frac{J_Z}{J_0}}, \tag{2.5}$$

where the parameters F_0 and ω_0 follow from formulas (2.1) and (2.3), J_0 is the ionization potential for the hydrogen atom in the ground state, and J_Z is the ionization potential for an ion of charge Z. The smallness of the Keldysh parameter

$$\gamma \ll 1 \tag{2.6}$$

allows the interaction between a laser electromagnetic wave and an atomic system to be determined by the wave electric field. A specific character of this interaction can be analyzed within the framework of this interaction regime. Note that in spite of the large amplitude of the electromagnetic wave, its interaction with an atomic system holds a nonrelativistic character. Indeed, a typical velocity of valence atomic electrons is on the order of the atomic velocity $e^2/\hbar$, and for atomic ions of a charge $Z \sim 1$ a typical electron velocity $v \sim Ze^2/\hbar$ has the same order of magnitude. Therefore, the parameter v/c, where c is the speed of light, is small, and this circumstance determines the nonrelativistic character of interaction of an electromagnetic field with the atoms and ions under examination.

When the strength of a laser field becomes comparable to that of the field of the atomic core, the atomic system under consideration is reconstructed. Then the rate of nonresonant multiphoton processes is comparable to the rates of resonant processes, though typical times of these processes become larger than atomic times [15]. A subsequent increase in the laser wave intensity may lead to over-barrier ionization of valence electrons. We will demonstrate below that an over-barrier transition of valence electrons to space regions where an electron becomes free after field switching off (the Bethe mechanism) is among the most efficient mechanisms of absorption of a strong electromagnetic wave at the first stage of its interaction with an atomic system [16].

In analyzing the behavior of valence electrons of the atoms and atomic ions in the field of an electromagnetic wave, it is convenient to compare it with the behavior of free electrons. A typical amplitude of oscillations of free electrons in the field of a laser wave is on the order of

$$a = \frac{eF}{m_e\omega^2}\,, \tag{2.7}$$

and is large in comparison with the Bohr radius a_0 if criteria (2.3) and (2.6) hold true. For example, if the electric field strength of an electromagnet wave is $F = 10^{18}$ V cm^{-1} and the wavelength is $\lambda = 0.8$ μm (the wavelength of the titanium–sapphire laser that is used most often as a source of femtosecond laser pulses), this parameter amounts to

$$a \approx 1500a_0 = 82 \text{ nm}\,. \tag{2.8}$$

Similar radius corresponds to a metal cluster consisting of approximately 10^8 atoms.

An atomic gas is not suitable as a target for a laser electromagnetic wave. Indeed, at a low concentration of atoms the electrons oscillate in the field of a laser wave only, and interaction with an atomic core is weak most of the time, which leads to a weak wave absorption. On the other hand, if the atomic concentration is high, even single ionization of atoms can lead to the critical electron density with respect to absorption of an electromagnetic signal, and the electromagnetic wave cannot penetrate deeply into a plasma. Therefore, in creating a plasma with a high temperature under the action of a short high-power laser pulse, one has to use a cluster or macroscopic atomic system as a target. It is necessary in the latter case to establish additional conditions in order to provide interaction of laser radiation with a restricted number of atoms.

2.2 Cluster ionization by a strong electromagnetic wave

Cluster ionization under the action of a laser pulse may be divided into inner ionization, i.e., ionization of cluster atoms and ions, and outer ionization, i.e., ionization of a cluster as a whole. In considering both ionization processes, we assume their over-barrier character. We utilize for this aim the Bethe model which, in spite of its roughness, allows us to understand the ionization character and to find the dependence of the parameters of the ionization process on electromagnetic wave parameters.

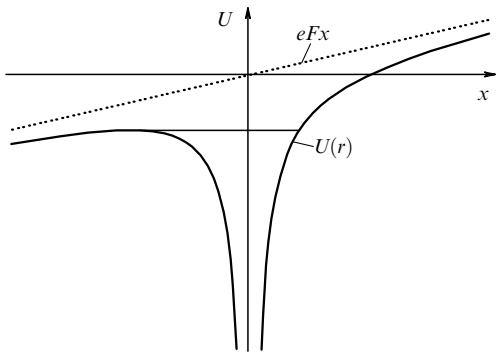

Figure 1. The electric potential acting on a released electron of a cluster atomic ion and created by the Coulomb field of the atomic core and instantaneous electric field of a laser electromagnetic wave.

In considering the ionization of an atomic particle in the field of an electromagnetic wave, we assume for simplicity that the released electron is located in the Coulomb field of an atomic core and the electromagnetic wave does not change the ionization potential of an atomic particle. Then the electric potential that acts on a released electron (see Fig. 1) is equal to

$$U = -\frac{Z}{r} + Fx\,, \tag{2.9}$$

where r is the electron distance from the atomic core, x is a coordinate along the field, Z is the atomic core charge, and F is the instantaneous electric field strength. This gives the barrier coordinate

$$x_0 = -\sqrt{\frac{Z}{F}}\,. \tag{2.10}$$

From this we find that over-barrier electron release takes place on meeting the criterion [10, 16]

$$F > \frac{J^2}{4Z}\,, \tag{2.11}$$

where J is the ionization potential of an atomic particle.

In particular, using the ionization potential of the hydrogenlike ion ($J = Z^2J_0/n^2$, where J_0 is the ionization potential of the hydrogen atom in the ground state, n is the principal quantum number, and this relationship is valid for large charges Z of an atomic core), we obtain for the maximum ion charge formed under the action of an electric field with the strength F:

$$Z = n^{4/3}\left(\frac{F}{F_0}\right)^{1/3}\,, \tag{2.12}$$

where the parameter F_0 is given by formula (2.1). In spite of the roughness of formula (2.12), it allows one to estimate the dependence of a charge of forming ions on the electric field strength.

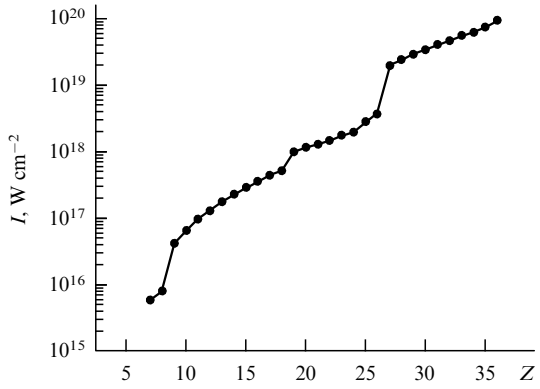

Figure 2. The dependence on the laser pulse intensity for a charge Z of a xenon ion in a cluster plasma resulting from excitation of a xenon cluster beam by a laser pulse.

Table 2. The ionization potential of xenon atom and ions.

Electron shell	J, eV	Electron shell	J, eV	Electron shell	J, eV
$5p^6$	12.13	$4p^6$	549	$3p^6$	2554
$5p^5$	21.21	$4p^5$	583	$3p^5$	2639
$5p^4$	32.1	$4p^4$	618	$3p^4$	2728
$5p^3$	46.7	$4p^3$	651	$3p^3$	2812
$5p^2$	59.7	$4p^2$	701	$3p^2$	2979
5p	71.8	4p	737	3p	3071
$5s^2$	92.1	$4s^2$	819	$3s^2$	3245
5s	105.9	4s	897	3s	3334
$4d^{10}$	171	$3d^{10}$	1385	$2p^6$	7663
$4d^9$	202	$3d^9$	1491	$2p^5$	7839
$4d^8$	233	$3d^8$	1587	$2p^4$	8143
$4d^7$	263	$3d^7$	1684	$2p^3$	8381
$4d^6$	294	$3d^6$	1781	$2p^2$	8987
$4d^5$	325	$3d^5$	1877	2p	9257
$4d^4$	358	$3d^4$	1987	$2s^2$	9582
$4d^3$	390	$3d^3$	2085	2s	9813
$4d^2$	421	$3d^2$	2211	$1s^2$	40,245
4d	452	3d	2302	1s	41,211

The important peculiarity of this process is a stepwise dependence of the ionization potential on the ion charge. Jumps in the ion ionization potential correspond to a change in the principal quantum number of a released electron. This fact is demonstrated by the data presented in Table 2, where the ionization potentials of xenon ions are compiled [17]. Such a behavior of the ionization potential determines the dependence of the charge of a forming ion on the intensity of an electromagnetic laser wave, in accordance with formula (2.12). This dependence contains plateau-shaped elements of the curve for ion charge values when the principal quantum number is kept constant, and it is illustrated in Fig. 2.

The example of a xenon cluster plasma resulting from the action of a strong electromagnetic wave on xenon atoms demonstrates the peculiarities of multiple atomic ionization in the electric field of an electromagnetic wave. The ionization process runs during atomic times, i.e., instantly on the scales under consideration, and the degree of ionization is determined by the wave electric field strength, so that this process for maximum ionization proceeds substantially at the instants of time when the harmonic wave field reaches maxima. Increasing the wave intensity results in a rise in the charge of the ion formed. Release of new electrons within the boundaries of one electron shell occurs monotonically at a not large change in the electromagnetic wave intensity, whereas passage to ionization of a subsequent electron shell requires an essential increase in the wave intensity. In particular, for xenon within the framework of the Bethe model, transition from the 5s to 4d electron shell requires an increase in the electromagnetic wave intensity by 5.3 times (from 7.9×10^{15} to 4.2×10^{16} W cm^{-2}), and the same increase in the electromagnetic wave intensity (from 3.8×10^{18} to 2.0×10^{19} W cm^{-2}) is required for transition from the 4s to 3d electron shell. Transition from the 3s to 2p electron shell requires an increase in the electromagnetic wave intensity by 26 times (from 2.6×10^{20} to 6.8×10^{21} W cm^{-2}). Next, within the framework of the Bethe model, in the laser intensity range under consideration, $I = 10^{16} - 10^{19}$ W cm^{-2}, the ion charge in a xenon plasma formed lies in the range of $Z = 9 - 26$.

In considering outer cluster ionization as a process of interaction between cluster electrons and an electromagnetic wave, we shall use again the Bethe model for determining the cluster charge. Assuming for simplicity a uniform electron distribution inside the cluster [10, 11, 18], we find the electric potential of the cluster with a charge Q:

$$U_{\rm cl}(r) = \begin{cases} -\dfrac{Q}{2R}\left(3 - \dfrac{r^2}{R^2}\right), & r \leqslant R, \\ -\dfrac{Q}{r}, & r \geqslant R. \end{cases} \tag{2.13}$$

Here, R is the cluster radius, and r is the distance from the point considered to the cluster center. By analogy with inner ionization, we find the barrier coordinate and, taking the electron energy Q/R at the cluster periphery as the cluster ionization potential, obtain the relation between the cluster charge Q and the electric field strength F:

$$Q = 4FR^2. \tag{2.14}$$

Expressing the cluster radius through a number of cluster atoms n as $R = r_{\rm W} n^{1/3}$, where $r_{\rm W}$ is the Wigner – Seitz radius [19], we reduce formula (2.14) for the cluster charge to the form

$$Q = 4Fr_{\rm W}^2 n^{2/3}. \tag{2.15}$$

Electrons that are released as a result of the ionization of cluster atoms and atomic ions under the action of the laser field are locked inside the cluster due to a self-consistent cluster electric field. Let us denote by α the fraction of electrons that leave the cluster on the basis of the formula

$$\alpha = \frac{Q}{Zn}, \tag{2.16}$$

where Z is the average charge of atomic ions, and n is the number of cluster atoms. This parameter ranges over $0 \leqslant \alpha \leqslant 1$, and in the limit $\alpha = 1$ all the electrons leave the cluster, while in the other limiting case $\alpha = 0$ all the electrons remain inside the cluster. Using formula (2.15) for the hydrogen atom in the ground state, one can represent formula (2.16) in the form

$$\alpha = \left(\frac{8F}{F_0}\right)^{2/3} \frac{r_{\rm W}^2}{a_0^2 n^{1/3}}. \tag{2.17}$$

Table 3. The degree of ionization α of a xenon cluster at different numbers n of cluster atoms and laser radiation fluxes I.

I, W cm^{-2} \ n	10^3	10^4	10^5	10^6
10^{16}	0.71	0.33	0.15	0.071
10^{17}	1	0.75	0.35	0.16
10^{18}	1	1	0.65	0.3

It is clear that if this formula gives $\alpha > 1$, then it is necessary to take $\alpha = 1$ during further computation.

As follows from formula (2.17), the degree of cluster ionization in the given electric field drops with an increase in cluster size. This is also demonstrated by the data compiled in Table 3 for xenon clusters consisting of different numbers n of atoms and at different intensities I of the laser pulse [18]. In considering the ionization of a cluster and its atoms by an electromagnetic field of laser radiation, we assumed implicitly that ionization proceeds instantaneously at the point in time when the electric field strength reaches the corresponding maximum. This is based on the assumption that the typical time of the over-barrier electron transition is small compared to the laser field period, so that ionization proceeds in a quasistationary electric field, i.e., when the Keldysh parameter is small. All this would hold for ionization of cluster atoms and atomic ions, but requires an additional analysis in the case of ionization of a cluster as a whole. If the ionization potential of the cluster as a whole is taken to be Q/R, in view of formula (2.14) the Keldysh parameter (2.5) takes the form

$$\gamma = \left(\frac{8R}{eF/m_e\omega^2}\right)^{1/2} . \tag{2.18}$$

From this it follows that ionization of a cluster as a whole can be considered an instantaneous process, if the cluster size does not exceed the amplitude of oscillations of a free electron in the laser field.

We assumed above that ionization of cluster atoms and ions is caused by an external electric field alone, irrespective of a self-consistent cluster field due to a noncompensated ion charge inside the cluster. In reality, a self-consistent cluster field, being summed with a laser field, intensifies ionization of cluster atoms. In particular, for a uniform charge distribution inside the cluster and according to formula (2.13), the electric field strength of the self-consistent cluster field is equal inside the cluster ($r \leqslant R$) to

$$F_{cl}(r) = \frac{dU_{cl}}{dr} = \frac{Q}{R^3}\, r = 4F\,\frac{r}{R} . \tag{2.19}$$

This field is zero at the cluster center, and is nonzero at the cluster boundary. Correspondingly, the charge of atomic ions on the cluster periphery is higher than that at the cluster center. In particular, drawing the analogy between ionization of a cluster as a whole and ionization of a hydrogenlike ion in the ground state, we find for the atomic ion charge Z depending on its distance r from the cluster center the following expression

$$Z(r) = Z_0\left(1 + 4\,\frac{r}{R}\right)^{1/3} , \tag{2.20}$$

where Z_0 is the ion charge at the cluster center. From this formula it follows that the ion charge at the cluster boundary is $5^{1/3} = 1.7$ times more than that at the cluster center. As a demonstration of this fact, Table 4 compares ion charges at cluster centers and at the boundaries (in parentheses) for real clusters [18] consisting of $n = 10^6$ atoms.

Table 4. Charges of atomic ions in some clusters located in a laser radiation field.

Ion \ I, W cm^{-2}	10^{17}	10^{18}	10^{19}
Kr	12 (18)	18 (26)	24 (27)
Xe	11 (24)	19 (28)	26 (43)
Mo	12 (14)	14 (24)	22 (32)
W	12 (38)	22 (47)	41 (56)

Note that electrons captured by a self-consistent laser field oscillate harmonically in this field and travel over the whole cluster volume. The oscillation frequency for the harmonic potential (2.13) is given by

$$\Omega^2 = \frac{Q}{m_e R^3} = \frac{4eF}{m_e R} . \tag{2.21}$$

Using formula (2.16), we obtain

$$\Omega^2 = \frac{Z\alpha}{m_e r_W^3} . \tag{2.22}$$

As can be seen, the frequency of electron oscillations in the self-consistent cluster field is comparable to a typical atomic value and usually exceeds the frequency of a laser electromagnetic wave, in particular, for a titanium–sapphire laser with a wavelength of about 0.8 μm, which is used as the primary source of femtosecond high-power laser pulses. According to the criterion $\Omega \gg \omega$, electrons propagate over the cluster volume fast and establish identical conditions in different cluster regions.

2.3 Character of absorption of laser radiation by a cluster plasma

In considering ionization of cluster atoms and ions, as well ionization of a cluster as a whole, we singled out the over-barrier transition of electrons as a fast process of interaction between a cluster and electromagnetic laser field. Then we assumed implicitly that an electromagnetic wave penetrates inside the cluster. Let us consider this process from the standpoint of a classical plasma. The wave cannot penetrate inside a uniform plasma if the frequency ω_p of plasma oscillations exceeds the electromagnetic wave frequency ω. Table 5 shows the frequencies ω_p of plasma oscillations and the boundary wavelengths λ_b for electromagnetic waves, so that longer waves cannot penetrate inside the plasma with a given density.

Table 5. Plasma oscillation frequencies ω_p and boundary wavelengths λ_b for an electromagnetic signal penetrating a uniform plasma of a given number density N_e of electrons.

N_e, cm^{-3}	10^{20}	10^{21}	10^{22}	10^{23}
ω_p, s^{-1}	5.6×10^{14}	1.8×10^{15}	5.6×10^{15}	1.8×10^{16}
λ_b, μm	3.4	1.1	0.34	0.11

Note that we are dealing with a dense plasma. For example, in the case of xenon (the Wigner–Seitz radius

equals $r_W = 2.37$ Å), the number density of ions is $N_i = 1.7 \times 10^{21}$ cm^{-3}, and since ions are multiply charged, the number density of electrons is accordingly higher. A weak electromagnetic signal penetrates in such a plasma to a depth on the order of the Debye – Hückel radius r_D, which is rather small. For example, the Debye – Hückel radius of a plasma with the electron number density $N_e = 10^{22}$ cm^{-3} and the electron temperature $T_e = 100$ eV amounts to 0.5 nm. This gives $N_e r_D^3 = 2$, so that this approach is not entirely adequate, and electrons must be considered as a degenerate electron gas at zero temperature. But this conclusion relates to a weak wave only.

A strong electromagnetic wave acts in another way. First, screening of a weak wave originates from displacement of boundary electrons which create a field that compensates for the wave field. But these electrons cannot create a strong field, which requires the participation of a large number of electrons in the screening process. As a result, a strong wave penetrates to a plasma more deeply. Second, electrons oscillate in the field of a strong wave; the amplitude of these oscillations can be large according to formula (2.7) and may be considered as the penetration depth of an electromagnetic wave into a plasma. Correspondingly, an electromagnetic wave penetrates inside a cluster whose radius is comparable to the amplitude of oscillations (2.7) for free electrons in the wave field:

$$R \sim a\,. \tag{2.23}$$

This estimate gives the typical size of the cluster to whose interior a strong electromagnetic wave can penetrate, with the extraction of electrons from its volume. Table 6 contains values of the oscillation amplitude for a free electron located in the field of a laser wave of a titanium – sapphire laser with the wavelength $\lambda = 0.8$ μm. Numbers of cluster atoms are also given in this table for clusters whose radius is equal to the oscillation amplitude of a free electron.

Table 6. The oscillation amplitude (2.7) for a free electron in the field of a laser wave and the number of cluster atoms.

I, W cm^{-2}	10^{16}	10^{17}	10^{18}	10^{19}
a, nm	8.7	28	87	280
n	1×10^5	4×10^6	1×10^8	4×10^9

As follows from the data presented in Table 6, a laser pulse penetrates deep into clusters of the size under consideration. But this penetration proceeds in a specific way, so that an electromagnetic wave inside the cluster mixes with plasma oscillations. Nevertheless, the above simple models describe qualitatively the character of ionization of cluster atoms and ions, as well as a cluster as a whole.

Thus, a partial plasma blooming takes place under the action of a strong electromagnetic wave, and this plasma is excited by hybrid waves which are a mixture of the electromagnetic wave and collective oscillations of the cluster plasma. Let us analyze also the role of collision processes involving electrons and ions of the cluster plasma. The diffusion cross section of electron – ion collisions due to the Coulomb interaction diverges at small scattering angles. According to the character of scattering in the cluster plasma, it can be cut off at collision impact parameters which are on the order of the Wigner – Seitz radius r_W [19], which corresponds to the minimum scattering angle:

$$\sin\left(\frac{\theta_{\min}}{2}\right) = \left(1 + \frac{4\varepsilon^2 r_W^2}{Z^2 e^4}\right)^{-1/2},$$

where Z is the ion charge, and ε is the electron kinetic energy. This gives the following expression for the diffusion cross section σ^* of electron – ion scattering in the cluster plasma:

$$\sigma^* = \int (1 - \cos\theta)\, d\sigma = \frac{\pi Z^2 e^4}{\varepsilon^2} \ln\left(\frac{2\varepsilon r_W}{Z}\right). \tag{2.24}$$

This formula is valid for large values of the parameter

$$x = \frac{2\varepsilon r_W}{Z} \gg 1\,, \tag{2.25}$$

which allows us to represent the diffusion cross section of electron – ion scattering in the cluster plasma in the form

$$\sigma^* = \frac{4\pi r_W^2}{x^2} \ln x\,. \tag{2.26}$$

From this it follows that for the mean free path λ of electrons in the cluster plasma we have

$$\lambda = \frac{1}{\sigma^* N_i} = \frac{x^2}{3 \ln x}\, r_W\,, \tag{2.27}$$

where $N_i = 3/(4\pi r_W^3)$ is the ion number density in the cluster. Table 7 contains the ratios λ/R of the electron mean free path in the cluster plasma with respect to its scattering on ions to the xenon cluster radius at some cluster sizes and intensities of the laser electromagnetic wave [20]. These data demonstrate that electron – ion collisions are of minor importance for establishing equilibrium conditions for cluster plasma electrons residing in the self-consistent cluster field and laser radiation field.

Table 7. The ratio of the electron mean length in a xenon cluster plasma to the cluster radius.

I, W cm^{-2} \ n	10^4	10^5	10^6
10^{16}	50	95	180
10^{17}	90	220	420
10^{18}	—	650	1800

The fastest process of interaction between a cluster and a strong electromagnetic wave is ionization of cluster atoms and ions as a result of the over-barrier transition of valence electrons in states of a continuous spectrum. This occurs at the points in time when the electric field strength of the wave reaches a maximum, and after a subsequent decrease in the electric field strength an atomic particle is found in an ionized state. Hence, the energy of an electromagnetic wave is spent on the ionization of cluster atoms and atomic ions. According to the character of electron behavior, we assume a prompt electron transition, i.e., it proceeds during atomic times which are small compared to oscillation times of an electromagnetic wave. As a result, the electromagnetic wave energy is expended on ionization of cluster atoms and ions.

But we encounter a contradiction when considering the electromagnetic wave absorption from another standpoint.

Indeed, a time that exceeds the period of electromagnetic oscillations is required for transformation of electromagnetic wave energy into the energy of a forming plasma. Therefore, absorption of electromagnetic wave proceeds more or less uniformly in the course of the total time of cluster irradiation. In order to bring this inference into agreement with the above scheme of ionization, it is necessary to assume that the wave does not penetrate to the cluster's interior and interacts with a small part of the cluster atoms and ions. The electrons formed move inside the cluster and establish an equilibrium between different cluster parts. Hence, the equilibrium inside the cluster plasma results from a sum of elementary and collective processes. Moving from the region of action of the electromagnetic wave to regions which are unavailable for the electromagnetic wave, electrons transform the electric potential acquired from the electromagnetic wave into kinetic energy. Since a transient region that is responsible for energy transfer is formed as a result of plasma collective processes, the absorbed energy is partially transformed to collective degrees of freedom, and then reverts to individual electrons.

Thus, a basis for the absorption of a strong electromagnetic wave by a cluster is provided by ionization of cluster atoms and ions as a result of over-barrier transitions of valence electrons under the action of the electromagnetic wave field. Propagation of electrons formed inward the cluster and their interaction with plasma collective degrees of freedom in the electromagnetic wave field lead to transfer of the energy of the electromagnetic wave into the energy of a forming plasma.

Let us find the rate of establishment of the equilibrium energy distribution for plasma electrons that is determined by electron–electron collisions. The Rutherford formula for the differential scattering cross section of two electrons in the center-of-mass system has the form [21]

$$\mathrm{d}\sigma = \frac{\pi e^4}{\varepsilon(\Delta\varepsilon)^2}\,\mathrm{d}\Delta\varepsilon\,, \tag{2.28}$$

where $\varepsilon = m_e v^2/2$ is the electron energy in the center-of-mass system, so that v is the relative electron velocity, and $\Delta\varepsilon$ is the energy change for electrons in the center-of-mass frame of coordinates. Hence follows the balance equation for the energy ε of a test electron:

$$\frac{\mathrm{d}\varepsilon}{\mathrm{d}t} = N_e v \int \Delta\varepsilon\,\mathrm{d}\sigma = N_e v\,\frac{\pi e^4}{\varepsilon}\int\frac{\mathrm{d}\Delta\varepsilon}{\Delta\varepsilon} = N_e\,\frac{\pi e^4}{m_e v}\ln\Lambda\,. \tag{2.29}$$

Here, N_e is the electron number density, and $\ln\Lambda$ is the Coulomb logarithm. Equation (2.29) allows us to estimate the typical time for the establishment of the Maxwell electron distribution in a cluster plasma. Its values are given in Table 8 for some cluster sizes and intensities of laser radiation [22]. According to the data of this table, a typical time of establishment of the Maxwell distribution for electrons significantly exceeds the duration of the laser pulse and typical times of cluster plasma expansion. Therefore, we are dealing with a nonequilibrium plasma whose parameters are determined by the conditions of its formation. The above character of interaction between a cluster beam and a short high-power laser pulse permits one to deposit a high specific energy into the electron subsystem, and this energy can reach ~ 1 keV per electron. Thus, absorption of energy of a high-power laser pulse by a cluster beam leads to the formation of a specific hot plasma.

Table 8. Typical times (ps) for establishing the Maxwell energy distribution for electrons in a cluster plasma formed under the action of a laser pulse.

I, W cm^{-2} \ n	10^4	10^5	10^6
10^{16}	9.5	30	95
10^{17}	26.4	84	264
10^{18}	—	470	1500

2.4 Mechanisms of interaction between a strong electromagnetic wave and a cluster plasma

In analyzing cluster interaction with a strong electromagnetic wave whose frequency is remarkably lower than the typical atomic frequency and the electric field strength exceeds the typical atomic value, we took as a model the over-barrier ionization of cluster atoms and ions in the wave electric field (being considered as the fastest process). This mechanism allowed us to formulate the character of interaction between a cluster and the electromagnetic wave field and analyze cluster evolution in the course of this interaction. But this approach relates to only one aspect of the problem, though this aspect is one of principle, whereas in general the possibilities of this approach are restricted. First, in such a consideration we assume implicitly that the wave penetrates freely to the interior of the cluster, which requires a specific analysis. Second, absorption of wave energy takes place in the course of ionization of cluster atoms and ions, so that the wave is damped, which is not taken into account within the framework of the above approach. But if we introduce these factors into the above consideration, the model of interest loses its simplicity and clarity. Accounting for these factors not only makes the description of the regimes of interaction more difficult, but also leads to a gap between this model and actual circumstances. Therefore, we advisedly used a qualitative description of the one aspect of interaction between a strong electromagnetic wave of a finite duration with an atomic system by extracting the fastest process of this interaction.

Along with the above mechanism of interaction between an electromagnetic field and cluster that gives a qualitative description of the evolution of the system, other mechanisms of interaction become valid when forming free electrons interact with the electromagnetic wave field in the interior of the cluster. These mechanisms were analyzed under certain conditions, and we give below the conclusions following from such considerations.

A cluster plasma resulting from ionization of cluster atoms under the action of an incident strong electromagnetic wave is matter with specific optical properties that influence the character of propagation of an electromagnetic wave through this matter. For example, the self-focusing of a femtosecond laser pulse with the intensity of about 3×10^{17} W cm^{-2} was demonstrated for a cluster beam of argon [23]. This effect causes strong absorption of the laser wave (up to 50%).

Computer simulation of cluster interaction with a strong electromagnetic wave is problematic because this process relates to a quantum system. Nevertheless, a classical description of cluster electrons provides a rough idea of the process. In particular, simulation of cluster electrons and ions by the classical method of molecular dynamics was carried out in Ref. [24] for excitation of xenon clusters comprising from 100 to 1000 atoms by a strong laser pulse. In this case,

the electron behavior is described adequately by the model of the harmonic oscillator with damping. Nonlinear resonant absorption on the back front of a femtosecond laser pulse is the basic mechanism for energy transfer from the laser pulse to cluster electrons.

Interaction of a weak electromagnetic signal with a metal particle may be considered a resonant wave interaction with surface plasma oscillations of a drop of metal. This mechanism was taken as the basis [25] for evaluating the heating of argon clusters by a femtosecond laser pulse with intensities ranging from 10^{15} up to 10^{16} W cm^{-2}. As a result of nonlinear resonant absorption, the electrons acquire a kinetic energy of several keV per electron on the back front of the femtosecond laser pulse, when the cluster starts to expand. The role of this mechanism was justified by experiment [26] where two laser pulses with a small time delay were utilized for the excitation of silver clusters embedded in helium nanodroplets. The second signal is used in this experiment for detection of the degree of atomic ionization. A similar conclusion about the role of resonant absorption of a laser pulse in the course of cluster expansion was demonstrated in experiment [27] where a beam of argon clusters of large sizes was irradiated by superintense laser pulses. On the fore-part of the front of the laser pulse, strong screening of the laser field by the cluster takes place because of high cluster permittivity. Basic electron heating occurs during cluster expansion at the points in time when the resonance between the laser wave frequency and plasma frequency of surface electrons is attained.

The resonant absorption of a laser pulse was intensified in experiment [28] by covering the surface of the irradiated target with a film of dielectric clusters, with the film thickness slightly exceeding the wavelength of the laser signal. Interaction of a laser wave with such clusters strengthens the resonant laser field on the cluster surface and causes a strong stochastic heating of electrons, which in turn leads to a marked increase in the efficiency of the X-ray yield.

The resonant of interaction under consideration is typical for metal clusters. In particular, evaluations [29] for sodium clusters with classical modeling of valence electrons and electrons of the inner electron shells interacting through the Coulomb law gave the threshold of cluster excitation on the order of 10^{16} W cm^{-2}, which corresponds to ionization of inner-shell electrons. The ion distribution over kinetic energies testifies to the cluster Coulomb explosion in a laser field. The average charge of forming atomic ions is close to 2 for the laser intensity indicated.

The analysis of the collisionless mechanisms of laser radiation absorption by cluster electrons [30] when, like the processes in Section 2.3, the frequency of plasma surface oscillations for the cluster is close to the frequency of laser radiation shows that the linear resonance is not generally realized. An increase in the laser intensity leads to emerging nonlinear resonances. The period of oscillations of an electron cloud located in the field of a strong electromagnetic wave increases due to nonlinear interaction, and this causes resonant absorption of a laser signal when the frequency of electron cloud oscillations becomes equal to the frequency of laser radiation [31].

The role of nonlinear absorption of a laser pulse by clusters comprising atomic particles was analyzed in Refs [32 – 34] when the resonance between the cluster plasma frequency and a triple frequency of the titanium – sapphire laser arises and disappears in the course of cluster expansion, with a cluster diameter being of approximately 10 nm, and the intensity of the femtosecond laser pulse on the order of 10^{16} W cm^{-2}. During the resonance, intensified atomic ionization takes place, leading to the formation of multiply charged atomic ions inside the cluster. Then, nonlinear oscillations of the electron cloud cause the generation of the second laser harmonic, i.e., an expanding cluster can be convenient matter for the generation of harmonics.

A cluster beam may be considered as medium with a time-varied effective permittivity that determines the character of propagation and absorption of a laser pulse. This approach, taking into account cluster expansion, shows the possibility of laser self-focusing in clusters under typical experimental conditions [35]. Complex cluster polarizability of inert gas clusters was calculated as a time function during their interaction with a femtosecond laser pulse [36]. It was demonstrated that the cluster interaction with a laser wave leads to a sharp change in the cluster medium polarizability during a laser pulse passage when the electron number density varies from subcritical up to above-critical values. The polarization cluster medium description may be useful when resonance interaction arises or disappears under certain conditions.

The field of a strong electromagnetic wave can remarkably change the parameters of a cluster plasma. This follows from calculations [37] performed by the cell method for classical relativistic electrons and ions that is applied to small xenon clusters excited by an excimer KrF laser with a wavelength of 248 nm and intensity up to 10^{21} W cm^{-2}. At the intensity exceeding 10^{20} W cm^{-2}, all the electrons were ejected from the cluster under laser irradiation. The electrons are accelerated up to an energy of several megaelectron-volts in the direction of laser pulse propagation. The laser magnetic field perturbs electron trajectories and causes a strong distortion of the electron cloud shape from the spherical shape, as takes place in weak laser fields.

Static dipole polarizabilities of dielectric nanoclusters were calculated in paper [38] using the polarizabilities of the atoms that compose the cluster. An employment of additivity approximation to atomic polarizabilities was found fallacious in many cases, and surface effects are of importance due to the action of the local inhomogeneous electric field near the surface.

The microscopic analysis of the explosion of large clusters in a strong laser field on the basis of the three-dimensional cell method shows that electron heating is determined by the electric field gradient in clusters [39]. This electric field results from outer cluster ionization, so that a cluster acquires some positive charge that is distributed over its volume, and the maximum electric field gradient is found on the cluster surface. The dynamics of cluster expansion are determined by an ambipolar electric field diffusion resulting from cluster – laser field interaction, as follows from cluster simulations by the cell method [40].

The analysis of profiles of Layman spectral lines of the hydrogenlike O^{7+} ion resulting from irradiation of N_2O clusters by femtosecond laser pulses with an intensity of 4×10^{17} W cm^{-2} exhibits the presence of strong oscillating electric fields with strengths of the order of 10^9 V cm^{-1} and frequencies of the order of 10^{15} s^{-1} [41]. Evidently, they occur due to quasistatic magnetic fields resulting from the Weibel instability.

In considering a spatial profile of a laser pulse irradiating the cluster beam and the saturation effect in cluster ionization

[42], it is noticed that in concrete calculations the interaction of a laser pulse with an individual cluster is examined, whereas in reality the interaction of a laser pulse with a cluster beam takes place.

Evaluation of the inner and outer ionization of xenon clusters with the number of atoms from 108 up to 524, irradiated by three intensive femtosecond laser pulses [43, 44], indicates how to optimize cluster ionization and collective oscillations of an electron cloud for understanding the character of the transition from small molecules to large clusters in inner and outer cluster ionization.

Debye screening by electrons decreases the ionization potentials of multicharge atomic ions in clusters of inert gases [45, 46] in comparison with the values relevant to isolated atoms. This is especially important for small electron temperatures. These calculations were substantially improved [47] by using the ionization potentials for a dense plasma with strong coupling. In addition, it was shown in Ref. [47] that the equality between the laser frequency and surface plasma oscillations does not establish optimal conditions for laser absorption because the resonance conditions are disturbed due to cluster heating and expanding.

The method of molecular dynamics was applied in Ref. [48] for calculating the inner and outer ionization of xenon clusters consisting of 2×10^3 atoms by laser pulses with an intensity of $10^{15} - 10^{18}$ W cm^{-2} and pulse duration from 10 up to 100 fs. Classical over-barrier ionization was taken into account along with impact ionization. The latter dominates for large clusters, low laser intensities (below 10^{15} W cm^{-2}), and relatively long pulses (100 fs); in this conditions atomic xenon ions have a charge below $Z = 11$ at the cluster center. Conversely, over-barrier field ionization dominates on the cluster surface. As a result, two radial charge distributions of xenon atomic ions form inside a cluster at small intensities of laser radiation. At high intensities of the laser pulse ($10^{17} - 10^{18}$ W cm^{-2}), impact ionization is not essential. Ionization by a cluster quasistatic electric field appearing in ionization of the cluster as a whole was only observed for very short pulses.

An electromagnetic wave does not penetrate in the interior of a large cluster and its interaction with electrons takes place in a surface layer (similar to solids). Interaction with a strong wave can cause so-called vacuum heating [49–51] when a slow electron leaves a cluster and, acquiring near it the energy equal to ponderomotive one, then returns inwards the cluster. For a radiation intensity of 10^{19} W cm^{-2}, the electron ponderomotive energy can reach dozens of MeV, and in consequence the electron passes a thick layer without collisions. Within the framework of the harmonic oscillator model for a self-consistent cluster field it is shown that under certain conditions a cluster can become transparent for laser radiation [51]. This can lead to high threshold intensities for multiple inner ionization of clusters [49], in comparison with the above-considered Bethe model of over-barrier ionization.

Interaction of a xenon cluster consisting of 54 atoms with short pulses of laser radiation with wavelengths of 100 and 800 nm was investigated taking into account the over-barrier ionization, field ionization, and recombination processes [52]. Portions of energy spent on ionization and absorption are comparable for long and short pulses. It was revealed that impact ionization is not important in all cases, and the basic ionization mechanism is due to a quasistatic radial electric field that results from outer cluster ionization. Electron heating proceeds through stimulated inverse bremsstrahlung absorption for the wavelength of 100 nm, and through vacuum heating of electrons for the wavelength of 800 nm.

The above investigations relate to cluster interaction with a laser pulse of a small frequency compared to typical atomic frequencies because all experimental studies use the laser wavelength of 0.8 nm. The development of free electron lasers widens the range of interaction parameters and requires the analysis of cluster interaction with a laser field under other conditions. According to the theoretical analysis [53] of this interaction for laser wavelengths of 100 and 800 nm, variation of the wavelength changes the relative role of collisional and collective processes in a dense cluster plasma. A novel mechanism of interaction involving short-wave laser pulses generated by a free electron laser [54] consists in a many-particle recombination of electrons and ions with the formation of excited ion states and the subsequent ionization of these ions. This mechanism leads to a more effective energy transformation than stimulated inverse bremsstrahlung absorption.

The above studies of absorption of an intense laser pulse by a cluster beam do not give a unified simple description of this process, and rather lead to a variegated picture that testifies to a variety of mechanisms and processes which can dominate under certain conditions. These processes can be changed both depending on interaction parameters and in time in the course of the formation and evolution of the cluster plasma. Nevertheless, we note that the evolution of a cluster plasma starts from the over-barrier ionization of cluster atoms and ions in a field of a strong electromagnetic wave, being the fastest process for the formation of free electrons. This establishes certain conditions for a subsequent plasma evolution that can proceed through various channels.

2.5 Cluster evolution after excitation

Up to now we have been restricted by processes running at the instant of cluster excitation, however, from the standpoint of applications [10, 11] the evolution of a cluster beam is not stopped after a pulse ceases. The sequence of processes in a laser-excited cluster plasma and the appropriate hierarchy of times is as follows [55–58]. At the first stage of cluster irradiation, atoms and ions are ionized, and a part of the electrons leave the cluster which acquires a positive charge. Other electrons are captured by a self-consistent cluster field and remain inside the cluster. The cluster decays under the action of the positive ion charge and hydrodynamic pressure of captured electrons, and cluster expansion finishes when the plasma becomes uniform. Simultaneously with cluster expansion, a part of the electron energy is spent on increasing the ion kinetic energy and ion excitations which produce X-ray emission. The duration of the second stage of evolution varies from several dozen ps to several hundred ps, and after cluster expansion the typical ion energy remarkably exceeds the typical electron energy. Figure 3 exhibits typical times for

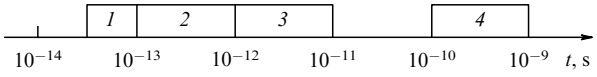

Figure 3. Typical times of processes accompanying excitation of a cluster beam by an ultrashort superintense laser pulse: *1* — laser pulse duration; *2* — cluster lifetime; *3* — time of uniform plasma formation after expansion of clusters; *4* — decay time for a uniform plasma.

the separate stages of the evolution of the plasma under consideration.

A typical duration of a laser pulse ranges 30 – 100 fs and is lower than the typical time of cluster expansion. Note that the opposite relation between these times for a hot plasma with multicharge ions leads to a low efficiency of excitation by laser radiation because it proceeds in a matter with a lower density. Hence, below we will consider expansion of a hot cluster plasma without the action of a laser pulse. There are two mechanisms of this plasma expansion: under the action of electron pressure, and under the action of a self-consistent cluster field, and both these mechanisms are determined by the character of interactions in this plasma.

This plasma is confined by a self-consistent cluster field that locks electrons inside the cluster, but this system is unstable with respect to ion motion. Hence, the lifetime of this plasma is determined by ion (not electron) times. Reflection of electrons from the walls of a self-consistent field and their return inwards the cluster creates a force that acts on the ions. Another force is determined by the action of a noncompensated cluster charge on the ions. Comparison of these forces [20] shows that the second mechanism usually dominates. Let us determine a typical time of cluster expansion on the basis of the ion mechanism. We have the following equation of motion for a test ion which at the beginning is located at a distance r from the cluster center:

$$M\frac{\mathrm{d}v}{\mathrm{d}t} = ZeF, \tag{2.30}$$

where M is the ion mass, Z is the ion charge, v is the ion velocity at a distance r from the cluster center, and F is the electric field strength at the point where a test ion is located. The last quantity is expressed through a cluster charge $Q(r)$ concentrated inside a sphere of radius r according to the Gauss theorem:

$$F = \frac{Q(r)}{4\pi r^2}, \tag{2.31}$$

where we assume a spherical symmetry of the charge distribution inside the cluster. This transforms equation (2.30) to the following form

$$M\frac{\mathrm{d}^2 r}{\mathrm{d}t^2} = \frac{ZeQ(r)}{4\pi r^2}. \tag{2.32}$$

Estimation gives the typical time of change of an ion distance from the cluster center:

$$\tau_{\mathrm{exp}} \sim \sqrt{\frac{Mr^3}{Q(r)Ze}}. \tag{2.33}$$

Relying on a given expansion mechanism and dividing the cluster into individual spherical layers, we arrive at the conclusion that in the course of cluster expansion these layers do not overlap and each layer will expand with an increase in the cluster radius. In the case of uniform charge density inside the cluster ($q = 3Q(r)/(4\pi r^3) = \mathrm{const}$), these layers will expand in a uniform manner. Then, the equation of motion (2.30) for a test ion takes the form

$$\frac{\mathrm{d}^2 r}{\mathrm{d}t^2} = \frac{r}{\tau_0^2}, \qquad \tau_0 = \sqrt{\frac{3M}{Zeq}}. \tag{2.34}$$

The solution of this equation is written down as

$$r(t) = r(0)\exp\left(\frac{t}{\tau_0}\right). \tag{2.35}$$

From this we find the ion velocity

$$v(t) = \frac{\mathrm{d}r}{\mathrm{d}t} = \frac{r}{\tau_0}. \tag{2.36}$$

It should be emphasized that ions are expanded in a space where free electrons are located, so that the total charges of electrons and ions in a plasma formed are identical. Correspondingly, the maximum distance in formula (2.36) holds to the Wigner – Seitz radius r_{max} of the cluster. This gives the maximum velocity v_{max} of an expanding cluster plasma:

$$v_{\mathrm{max}} = \frac{r_{\mathrm{max}}}{\tau_0} = \frac{3^{1/3}}{(4\pi N_{\mathrm{cl}})^{1/3}\tau_0}, \tag{2.37}$$

where N_{cl} is the number density of the clusters. This velocity determines the rate of ion processes in a forming plasma; in particular, it is responsible for the rate of fusion reaction in the case of a beam of deuterium clusters.

2.6 Experimental aspects of laser irradiation of cluster beams

Experiments on cluster excitation by an ultrashort superintense laser pulse exhibit the peculiarities of experimental technique. As an intermediate object between rarefied gaseous systems, on the one hand, and condensed atomic systems (solid or liquid), on the other hand, clusters experience a strong interaction with incident radiation, similar to condensed atomic systems (solids or liquids), which ensures a high specific energy input per atomic particle, like in gaseous systems [59, 60]. X-ray radiation of a forming plasma is a consequence of this phenomenon and can be used for the diagnostics of this plasma [4, 6, 61 – 63]. This is supported by the high efficiency of transformation of laser energy to the energy of X-ray radiation, which reaches 10% [8, 9] and offers possibilities of applying this experimental technique in lithography [64]. In addition, this method is used for neutron generation [65 – 68], thus increasing interest in this method and the experimental technique joined with specific diagnostics.

In analyzing the character of interaction between a laser pulse and cluster beam, we single out two limiting cases, so that for clusters of light elements the total ionization takes place for the cluster as a whole. The excitation of clusters of heavy elements leads to the formation of multicharge ions which confine electrons inside the cluster. In the case of total cluster ionization, one can expect a simplification of the problem because interaction of the laser field with a cluster terminates after cessation of ionizing and then cluster expansion results from Coulomb interaction of cluster ions with the cluster charge. But experimental studies of a hydrogen plasma resulting from irradiation of hydrogen clusters by laser pulses with a duration of 40 and 250 fs [69, 156] reveal an anisotropy in the angular distribution of taking-off protons. Moreover, an increase in pulse duration leads to an increase in the typical ion energy. From this it follows that a simple model [69] of cluster decay is inadequate for the determination of the energy distribution function of

protons in a forming plasma. Nevertheless, this simple model works well at lower intensities of laser pulses, as follows from experiments [70] with hydrogen clusters which were irradiated by a laser pulse with an intensity of 6×10^{16} W cm^{-2} that led to proton generation with an average energy of 8.1 keV.

During the excitation of a cluster beam of heavy elements by a laser pulse their interaction lasts the total irradiation time. The energy spectrum of ions and angular distribution of electrons were measured in Ref. [71] for xenon clusters consisting of 520,000 – 1,500,000 atoms and subjected to the maximum intensity $10^{15} - 10^{16}$ W cm^{-2} of laser radiation with a pulse duration of 100 – 2200 fs. According to these studies, cluster decay is described by the hydrodynamic model. In this case, the Maxwell distribution of electrons over energies corresponds to small clusters, while a two-temperature electron distribution relates to large clusters. The total electron current exhibits an asymmetric angular distribution that takes a resonance form at pulse durations above 1 ps. This points to a specific character of plasma evolution in the course of cluster expansion and allows one to analyze the role of different interactions in a decaying plasma.

The charge and energy distributions of xenon ions in an expanding plasma were measured for the intensity 2×10^{17} W cm^{-2} of a laser pulse with a duration of 500 fs [72]. The average energy of multicharge ions is 0.1 MeV, and the maximum cluster energy is 2 MeV at the positive frequency modulation of the laser pulse. It is of interest that the average energy of xenon ions at the negative frequency modulation is 1.6 times higher than that at the positive modulation.

X-ray emission from a krypton cluster laser-produced plasma was investigated in Ref. [73] using a laser pulse intensity of 1.3×10^{18} W cm^{-2}. The X-ray spectrum included strong krypton K_α and K_β lines that correspond to photon energies of 12.66 and 14.1 keV. This spectrum also included a wide continuous spectrum ranging up to 45 keV that testifies to the heating of about 10% of the electrons and confirms the two-temperature character of the electron energy distribution. The maximum efficiency of transformation of the laser energy to X-ray energy on the line 12.66 keV (K_α line) amounts to 9.2×10^{-7}, and the maximum energy on this line is 45 nJ.

Study of neonlike, fluorinelike and aluminiumlike krypton ions at the laser intensity 10^{19} W cm^{-2} and pulse duration 30 – 500 fs (the average energy is 50 – 300 mJ) [74] shows that the maximum of X-ray radiation is observed 1 – 2 ps after cessation of a pulse. The analysis of these findings gives a typical electron number density of 10^{22} cm^{-3} in this cluster plasma, and the electron energy of several hundred eV. In addition, excited neonlike krypton ions result from electron – ion collisions.

The evolution of the polarizability of a cluster plasma as the plasma's response to an optical signal [36, 75] allows us to study the dynamics of an expanding cluster plasma [76], since this plasma contains under-critical and above-critical regions for the propagating laser signal. At the reflecting boundary for a weak optical signal its frequency coincides with the plasma frequency of electrons in this region [77]. Additional information may be obtained from the measurement of spectral line shift as a result of the interaction of a laser pulse with a cluster plasma [78].

The above results of experimental investigations show that describing the interaction of an intense laser pulse with clusters is not exhausted by the simple models which were utilized earlier as a basis for this interaction. These models rely on the interaction of an electromagnetic wave with individual atomic particles, whereas in reality the penetration of an electromagnetic wave through a cluster also excites collective degrees of freedom, which raises the plasma nonuniformities. This causes specific effects which can change essentially the interaction character, and because of a variety of collective effects they act in a different manner depending on the cluster and electromagnetic wave parameters.

3. X-ray radiation of a cluster plasma at femtosecond excitation

3.1 Mechanisms of radiation of a laser-excited cluster plasma

The interaction of a cluster beam with a femtosecond high-power laser pulse can be used for creating an effective and compact source of X-ray radiation [2 – 5, 8, 79 – 89]. As a result of laser absorption, a nonuniform hot plasma is formed that consists of multicharge ions and electrons [10, 11, 55, 56]. The subsequent evolution of this plasma after cessation of the laser pulse creates multicharge ions and other excitations in a plasma, which leads to the emission of short-wave photons. Note that the possibility of emitting short-wave radiation is a property of any hot plasma, and the peculiarity of a given plasma is quickly passing through the excitation processes, so that the duration of the first stages of the evolution of this plasma is shorter than the time of photon emission. This determines the specifics of radiative processes, so that excitation is created at the first stages of plasma evolution, while photons appear at subsequent stages of its evolution. Nevertheless, this plasma provides a significant efficiency of transformation of laser energy into X-ray energy, which at wavelengths near 13.2 nm reaches $\sim 1\%$.

Let us consider the mechanisms of X-ray emission of a laser-excited cluster plasma [20], which include the processes of photorecombination, dielectron recombination, and excitation of multicharge ions by electron impact. Some processes typical for a stationary hot plasma were excluded from this list because of the short lifetime of the plasma under consideration. The photorecombination process proceeds according to the scheme

$$\mathrm{e} + A^{+Z} \rightarrow A^{+(Z-1)} + \hbar\omega\,. \tag{3.1}$$

This process can be effective until the cluster decays, when the plasma density is high. The cross section of this process is relatively small because it includes a small parameter $(e^2/\hbar c)^3$ that is responsible for the interaction of an electromagnetic wave with an atomic system [90 – 92], and at small electron velocities v this cross section is proportional to v^{-2}. Hence it follows that this process proceeds in a dense cluster plasma primarily near the turning points, when an electron captured by a self-consistent cluster field reflects from its walls. According to the theoretical prediction [20], the probability of photorecombination of a test electron during the lifetime of a cluster plasma under consideration is on the order of 10^{-5}.

Another mechanism of X-ray emission of a cluster plasma results from electron capture on the autoionizing level of a multicharge ion. Because the excitation energy for an autoionizing state is near the energy of a captured electron, this process exhibits a resonant character and proceeds

according to the scheme

$$e + A^{+Z} \to \left[A^{+(Z-1)}\right]^{**}. \tag{3.2}$$

Subsequently, the decay of the autoionizing state proceeds according to the following channels:

$$\left[A^{+(Z-1)}\right]^{**} \to e + A^{+Z}, \tag{3.3}$$

$$\left[A^{+(Z-1)}\right]^{**} \to \left[A^{+(Z-1)}\right]^{*} + \hbar\omega. \tag{3.4}$$

Here, Z is the ion charge, and $\left[A^{+(Z-1)}\right]^{**}$ is an autoionizing state of a multicharge ion. The analysis of the role of dielectron recombination in the decay of this cluster plasma shows the sensitivity of the process rate to the structure of multicharge ions and plasma parameters. If the typical energy of plasma electrons corresponds to the excitation energy of autoionizing states in multiply charged ions, the probability of dielectron recombination of a test electron during the plasma lifetime may be around unity [20]; in particular, this takes place in the case of dielectron recombination involving neonlike ions [93].

One more mechanism of emission of a laser-excited cluster plasma corresponds to the excitation of multicharge ions by electron impact and proceeds according to the schemes

$$e + A^{+Z} \to e + \left[A^{+Z}\right]^{*}, \tag{3.5}$$

$$e + \left[A^{+Z}\right]^{*} \to e + A^{+Z}, \tag{3.6}$$

$$e + \left[A^{+Z}\right]^{*} \to e + A^{+Z} + \hbar\omega. \tag{3.7}$$

The cross section of inelastic collisions of electrons with multicharge ions is decidedly less than that for elastic collisions [91, 92, 94], and an equilibrium between excited and unexcited states of multicharge ions in a plasma is not attained. Next, the quenching of excited multicharge ions lasts a long time in comparison with the times of plasma evolution, and therefore quenching of excited multicharge ions by electron impact is not essential. In addition, typical radiative times of multicharge ions are much long compared to the time of cluster expansion. Hence, excited multicharge ions are created before cluster decay, whereas their emission takes place at the following stages of plasma evolution. In addition, note that the efficiency of excitation of multicharge ions by electron impact is rather sensitive to the structure of the multicharge ion, as it is in the case of dielectron recombination.

Thus, the analysis of radiative mechanisms for a laser-excited cluster plasma reveals that the emission proceeds during the stage of a uniform plasma after cluster decay, being resulted from dielectron recombination and the radiation emission of excited multicharge ions which are formed from the excitation of multicharge ions by electron impact in clusters [20, 22]. The efficiency of emission of X-ray photons can reach several percent.

3.2 Radiation spectrum of a cluster plasma and its other peculiarities

The radiation spectrum of a laser-excited cluster plasma is determined by mechanisms of excitation of multiply charged ions which produce this radiation. Such a spectrum accompanies the kinetics of evolution of this plasma, which follows from certain calculations under certain conditions [95, 96]. Below we consider the basic peculiarities of plasma spectral properties on the basis of simple models [22, 95, 96].

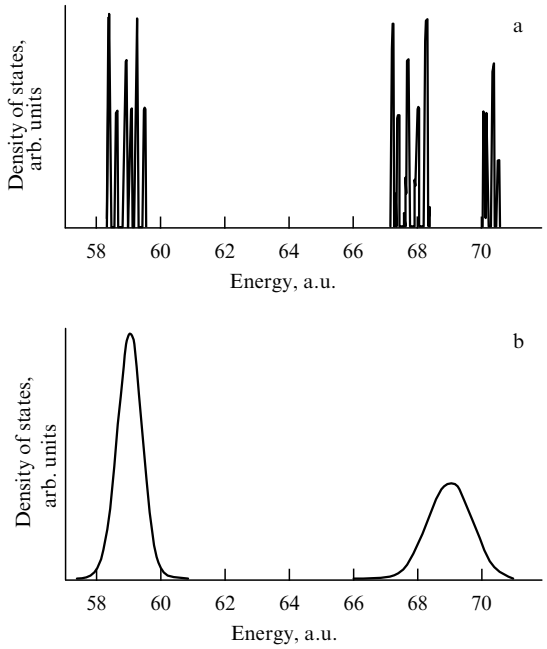

Figure 4. The density of states of Xe^{30+} ions for an isolated ion in vacuum (a) and for this ion located in a dense plasma (b).

It should be noted that the radiation spectrum of a long-lived hot dense plasma corresponds to the spectrum of a black body with the same temperature and is formed due to electron – ion collisions. The radiation spectrum of this short-lived plasma is connected with fast processes of particle excitation. Two primary processes cause X-ray emission of the plasma: dielectron recombination, and spontaneous radiation of excited multicharge ions. In both cases, the energy of emitted photons is determined by the energy difference between the autoionizing and final levels for dielectron recombination or the energy difference between the final and excited states for spontaneous radiation, i.e., the photon energy depends on the structure of ion levels. For a rarefied plasma, the width of these levels is small and neighboring levels do not overlap, i.e., the radiation spectrum of a rarefied hot plasma consists of separate discrete broad lines. In a dense plasma, the broadening of spectral lines due to the Stark effect leads to overlapping of neighboring spectral lines, and the spectrum forms a non-regular quasicontinuous structure (see Fig. 4). As a result, this spectrum consists of individual bands [22].

Thus, the radiation spectrum of a laser-excited cluster plasma consists of separate bands which are determined by the structure of ions and energies of their resonantly excited states, including autoionizing states. The continuous character of these bands follows from a strong broadening of individual spectral lines due to the high plasma density. A large number of transitions in the spectrum of this plasma allows one to use statistical methods for its analysis [97, 98]. Correspondingly, the form of this emission spectrum may be obtained on the basis of the statistical model [22] by using the density of states for levels participating in radiative transitions and the widths and positions of individual spectral lines for a given series [97 – 99]. Figure 5 gives an example of such a spectrum that is produced by xenon ions with a charge $Z = 32$, when this xenon plasma results from

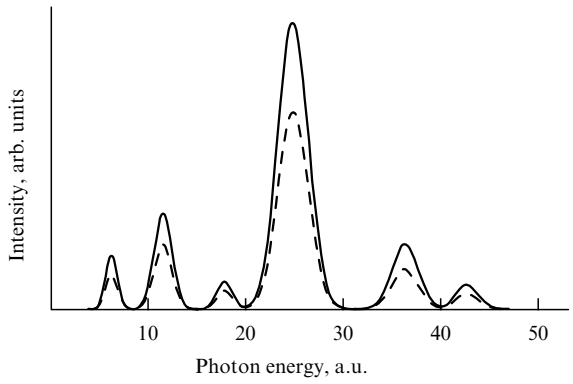

Figure 5. The radiation spectrum of a xenon cluster plasma at the electron temperature equal to fourfold ionization potential of Xe^{32+} ions (solid curve) and sixfold ionization potential of the same ions (dashed curve).

laser irradiation of xenon clusters consisting of 10^9 atoms. As is seen, the spectrum shape depends weakly on the plasma temperature [22].

A study of X-ray emission [100] produced in the course of irradiation of a beam of inert gas clusters consisting of 10^5 atoms by the ultrashort laser pulses of intensity 10^{15} W cm^{-2} testifies to a new mechanism of X-ray generation at small laser intensities. Elastic backscattering of electrons on ions under the action of a laser field, i.e., bremsstrahlung in the laser field, produces X-ray radiation.

A theoretical study of the dynamics of shock waves generated as a result of Coulomb explosion of deuterium clusters consisting of 10^6-10^7 atoms in a laser field of intensity 10^{18} W cm^{-2} was carried out by the cell method of relativistic particles [101]. Forming shock waves in an expanding cloud of deuterons increases the probability of a fusion reaction.

Investigation of the interaction of an intense femtosecond laser pulse with clusters consisting of a mixture of light atoms (deuterons) and heavy atoms [102] shows that a heavy component increases the probability of a fusion reaction by a higher electric potential of charged clusters. This is confirmed experimentally for a mixture of deuterium and methane in clusters.

In experiment [103], laser pulses with an intensity of 10^{17} W cm^{-2} and duration of 40 fs were applied to a beam of argon clusters with sizes from 180 up to 350 Å. Observed γ-radiation with photon energies from 2.9 to 4.3 MeV testifies to the formation of multicharge atomic ions of a high charge, up to Ar^{16+}, as a result of cluster Coulomb explosion. The mechanism of the formation of such ions has more of a collision nature than a field one.

Numerical calculations for the Coulomb explosion of hydrogen clusters irradiated by ultrashort intense laser pulses show that the maximum proton energy at a given laser intensity is attained at a certain cluster radius [104]. A two-dimensional cluster model [105] with typical parameters of laser pulses and clusters confirms that the mechanism of formation of fast ions results from cluster ionization as a whole. The pressure of an electron cloud inside the cluster is not essential for this process.

The measurement of energy spectra of argon ions [42] as a result of the Coulomb explosion of argon clusters at a laser intensity of 10^{17} W cm^{-2} exhibits a distinction from the theoretical dependence, which is $E^{1/2}$. A more weak experimental dependence is explained as the effect of cluster inner ionization. The thickness of the cluster surface layer that is responsible for the formation of fast ions is determined by the cluster field due to outer ionization.

A numerical analysis in Ref. [106] of experiments by T Ditmire and his colleagues on the irradiation of deuterium clusters with an intense femtosecond laser pulse shows that at small laser intensities a slow separation of a cluster charge proceeds, while high laser intensities (above 10^{15} W cm^{-2}) cause a Coulomb cluster explosion after the eruption of the greater part of electrons.

The excitation of hydrogen clusters by a femtosecond laser pulse of intensity 6×10^{16} W cm^{-2} causes their Coulomb explosion, and the energy distribution of the protons formed was registered in experiment [107]. The average proton energy was 8.1 keV, and the observed energy spectrum corresponded to a simple model for the expansion of a spherical uniform cluster. The maximum energy of protons depended both on the cluster size and on the laser intensity.

Theoretical analysis [108] of small clusters consisting of 16–30 rare gas atoms and interacting with an intense femtosecond laser pulse showed that the bulk of laser energy is absorbed during cluster expansion, when the distance between nearest ions increases by 30% in comparison with the initial distance. In addition, absorption of a laser radiation by clusters depends weakly on the polarization of radiation at the same laser intensity.

Interaction of xenon clusters with a femtosecond laser pulse with an intensity of 2×10^{17} W cm^{-2} was studied in Refs [72, 109] at a pulse duration ranging between 100 and 600 fs. The average energy of the xenon ions had a maximum of 500 keV at a pulse duration of 500 fs. The negative chirp modulation of the pulse led to ion energies around 60% higher than those at the positive chirp modulation.

The asymmetry in the angular distribution of high-energy electrons released in the outer ionization of xenon clusters comprising from 150,000 to 520,000 atoms was observed at an intensity of the laser pulse from 10^{15} up to 10^{16} W cm^{-2} and pulse duration from 100 fs to 2.2 ps [110]. Under these conditions, the dynamics of cluster expansion comply with the hydrodynamic regime caused by the pressure of electron gas inside the cluster. The maximum yield of electrons corresponded to a pulse duration of 1 ps. The laser field induces a polarization charge on the cluster surface that in turn creates an electrostriction force. The latter is comparable to the Coulomb and hydrodynamic forces, but has a resonant character. Resonant absorption of the laser energy by cluster electrons proceeds primarily in the low-energy part of the electron spectrum.

In the theoretical analysis [111] of the ionization of metal clusters with a strong laser pulse, where electron heating results from inverse bremsstrahlung, the thermal ionization of clusters and a field structure were taken into account. It was shown that at the pulse intensity of 10^{18} W cm^{-2} and the optimal radius of iron clusters equal to 25 nm, the electron temperature exceeds 1 keV and the electron L-shell of ions is ionized. X-ray emission results from bremsstrahlung, and the skin depth is less than the cluster radius.

Mechanisms of inner and outer cluster ionization in a strong electromagnetic field were analyzed in review [13]. The review compares the interaction of cluster beams with a laser pulse for both the standard wavelength of 780 nm and a new free electron laser with wavelengths ranging from 100 up to 3 nm (vacuum ultraviolet). The role of a spatial profile of a

laser pulse in its interaction with a cluster beam and the role of saturation in the ionization of clusters were analyzed theoretically in Ref. [112]. The authors have noted that these effects correspond to real conditions, whereas the interaction of one cluster with a laser field is usually taken into account in theoretical evaluations.

It is suggested in Ref. [113] that water be added to inert gas clusters in order to increase the yield of X-ray radiation produced upon their irradiation with femtosecond laser pulses. According to experiments, the addition of water to argon clusters increased the intensity of X-ray emission twelvefold. A possible reason for this increase is an intensification of inner cluster ionization due to H_2O molecules.

The interaction of hydrogen clusters with laser pulses of intensity 10^{16} W cm^{-2} and duration 65 fs was examined experimentally in Ref. [114]; investigations demonstrated a linear dependence of the proton kinetic energy on the square of the cluster radius. This fact unambiguously testifies to the Coulomb mechanism of cluster explosion; it was shown that this mechanism dominates for a cluster radius below 20 Å. Then inner ionization results from over-barrier electron transitions in the field of the laser wave.

3.3 Collision of cluster beams

The excitation of clusters in collisions of dense cluster beams is similar in nature to cluster excitation by an intense short laser pulse. As a result of cluster collisions, the kinetic energy of the clusters is transformed into their excitation energy. Though under contemporary capabilities of accelerating cluster beams this method is inferior to the laser method, it holds much promise for the excitation of matter. Excitation processes accompanying cluster collisions are analogous to those in the above method of cluster excitation by a laser radiation. In the course of cluster collisions, they form a joined cluster where the kinetic energy of the atoms is transformed to the excitation energy of the electron component. Part of the electrons leaves the cluster, and then a joined cluster expands into the surrounding space as a result of interaction between the ions moving inside it and a self-consistent cluster field. Finally, this leads to the formation of a uniform plasma that occupies all the space of the cluster beams. Subsequently, this plasma will also decay by expansion into the surrounding space.

The character of cluster collisions is determined by the interaction of cluster atoms with the matter where they are moving [115, 116]. This process depends on the collision velocity and the degree of cluster excitation during the collision. There are various models for describing the processes going on in the collisions (see, for example, Refs [117 – 122]). We will restrict ourselves below to simple models for the transformation of nuclear kinetic energy into electron excitation energy.

Let us consider the behavior of a test atom of one cluster that penetrates with a relatively large energy deep into another cluster. We assume the collision velocity to be large, so that the cross section of an atomic collision with surrounding atoms is small compared to the size of the atom. Then, atoms move inside the cluster matter independently, and their kinetic energy is converted into the energy of electron excitations. Thus, chemical bonds between atoms are broken in the course of cluster collisions, and atoms or ions of one cluster penetrate freely inwards the other cluster. Then, cluster excitation consists in the conversion of ion kinetic energy into the excitation energy of the electron subsystem. In the case of collisions of large clusters, as in collisions of clusters with the solid surface, the transformation of cluster kinetic energy becomes more complex and also includes the excitation of plasma oscillations and shock waves. In the case of cluster collisions, shock waves cannot be formed because of their small sizes. Along with the number $N_{\rm cl}$ of clusters in a beam and the number n of cluster atoms, a parameter of dense cluster beams is also the average number density $N_{\rm b}$ of bound atoms in the space that is connected with the above parameters by the relation

$$N_{\rm b} = nN_{\rm cl}\,. \tag{3.8}$$

Dense cluster beams involving atoms or molecules are usually generated by the free jet expansion of heated gases [123 – 131]. In this method, a gas or vapor is located in a chamber under a high pressure and flows from it through a nozzle. After the nozzle, the temperature of gas drops, and its atoms or molecules can join in clusters. This method of cluster beam generation is used for gases and vapors of lightly evaporated metals and materials. In the case of heat-resistant metals, dense cluster beams can be obtained from the flow of a hot plasma of the buffer gas into which weakly bound metal compounds are introduced [132 – 135]. This method provides high densities of metal cluster beams where the density of bound atoms is compared to that of cluster beams comprising gaseous atoms or molecules [134, 136]. In what follows we will be guided by a typical number density $N_{\rm b} = 3 \times 10^{19}$ cm^{-3} of bound atoms in dense cluster beams. Note, in particular, that the number density of deuterium atoms in the cluster beam that is used for neutron generation is $N_{\rm b} = (5-6) \times 10^{19}$ cm^{-3} [137, 138].

Figure 6 demonstrates the schematics of a collision of two cluster beams [136, 139]. For achieving strong interaction between cluster atoms, it is necessary that each cluster from one beam be able to collide with the atoms of another cluster beam. For definiteness, we take the nozzle as a narrow slot that enables generating a cluster beam of a rectangular shape. Assuming frontal or almost frontal collisions between clusters, we obtain the following criterion for a beam length L that provides collisions of individual clusters for small angles between colliding cluster beams:

$$N_{\rm cl}\sigma L \geqslant 1\,. \tag{3.9}$$

Here, $\sigma = 4\pi r_{\rm W}^2 n^{2/3}$ is the cross section of collisions of two identical clusters, so that $r_{\rm W}$ is the Wigner – Seitz radius for clusters. Passing to the number density $N_{\rm b}$ of bound atoms in the cluster beam according to formula (3.8), we represent criterion (3.9) in the form

$$4\pi r_{\rm W}^2 N_{\rm b} L \geqslant n^{1/3}\,. \tag{3.10}$$

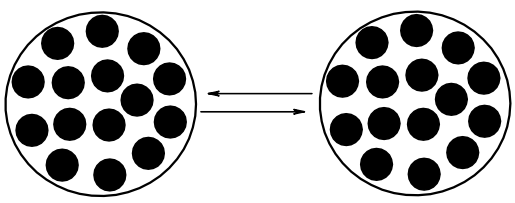

Figure 6. Collision of two cluster beams.

Criterion (3.10) specifies optimal conditions for cluster collisions. In particular, being guided by clusters of Mo, W, and Ir, with the value of the Wigner–Seitz radius equal to $r_W \approx 1.6$ Å [19], we obtain for $N_b \sim 3 \times 10^{19}$ cm^{-3} criterion (3.10) in the form

$$\frac{L}{n^{1/3}} \geqslant 10^{-5} \text{ cm} . \tag{3.11}$$

For the typical cluster size $n \sim 10^6$, criterion (3.11) gives $L > 10$ μm. This exhibits the possibility of realizing effective collisions of two cluster beams under real conditions.

3.4 Electron excitation in collisions of cluster beams

The collision of two clusters is accompanied by the mutual penetration of atoms deep into the clusters, where atoms and ions move inside the cluster matter and interact with it. Ion braking results from elastic collisions with other ions inside the clusters and from electron excitation. The second mechanism is dominant in a wide range of cluster and collision parameters. We consider below this mechanism of transformation of the ion kinetic energy.

We base our study of ion braking on a simple model, considering the electron subsystem as a degenerate electron gas. The momentum distribution function of electrons then corresponds to their location in the momentum space inside the Fermi sphere where the electron momentum is below p_F, namely, its radius. The cluster collision velocity v is small compared to the electron velocity v_F on the Fermi sphere surface:

$$v \ll v_F . \tag{3.12}$$

We consider each cluster in the course of its collisions to be divided into individual ions, so that each ion interacts with surrounding electrons and moves in the cluster's interior independently of other ions. Excitation of the electron subsystem then proceeds in pair ion collisions with electrons. Since the change in the electron momentum in collisions with the ion does not exceed $m_e v$, where m_e is the electron mass, and v is the ion velocity, criterion (3.12) gives $m_e v \ll p_F$, so that a small portion of electrons near the Fermi surface may partake in this process. For the majority of electrons this process is forbidden according to the Pauli exclusion principle, because the final electron state is occupied in these cases (see Fig. 7).

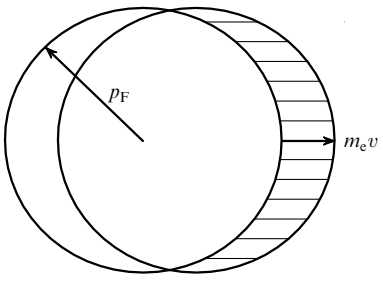

Figure 7. The character of electron transition for a degenerate electron gas resulting from electron collisions with ions moving inside the gas. The electron distribution of a degenerate electron gas in the momentum space is given before (nonshaded area) and after collision. Since an electron can only go to an unoccupied state, just electrons near the Fermi sphere can partake in the collision process (shaded region of the Fermi sphere).

Along with criterion (3.12), we assume the electron gas to be sufficiently dense, which gives the following small expansion parameter:

$$\alpha = \frac{e^2}{\hbar \pi v_F} . \tag{3.13}$$

In view of criterion (3.12), the first term of expansion of the braking rate over the small parameter (3.13) for a slow ion moving in a uniform, dense, degenerate electron gas has the following form [140, 141]

$$-\frac{d\varepsilon}{dx} = \frac{2Z\hbar v}{3\pi a_0^2}\left[\ln\left(\frac{4}{\alpha}\right) - 3 + 3\alpha \ln\frac{4}{\alpha} - \frac{11}{2}\alpha\right] = C(\alpha)\frac{Z\hbar v}{a_0^2} ,$$
$$C(\alpha) = \frac{2}{3\pi}\left[(1+3\alpha)\ln\left(\frac{4}{\alpha}\right) - 3 - \frac{11}{2}\alpha\right] . \tag{3.14}$$

Here, ε is the ion energy, x is the coordinate directed along the ion motion, Z is the effective ion charge during its motion with the velocity v inside the electron subsystem, e is the electron charge, and a_0 is the Bohr radius.

Let us examine the parameters of formula (3.14) for real clusters. Considering the electron subsystem as a degenerate electron gas, we have for the Fermi velocity of electrons

$$v_F = \frac{\hbar}{m_e}(3\pi^2 N_e)^{1/3} , \tag{3.15}$$

where N_e is the electron number density. Since each cluster atom gives Z electrons which interact with moving ions, we obtain

$$N_e = 2ZN_a , \tag{3.16}$$

where N_a is the atom number density for an isolated cluster. The factor 2 takes into account that mutual penetration of clusters leads to a doubling of the electron and ion number densities until a self-consistent cluster field influences their distributions. The atom number density N_a of an isolated cluster is connected with the Wigner–Seitz radius by the relation [19]

$$N_a = \frac{3}{4\pi r_W^3} . \tag{3.17}$$

This gives the expression for the electron number density:

$$N_e = \frac{3Z}{2\pi r_W^3} . \tag{3.18}$$

Substituting the electron number density (3.18) into formula (3.13), we arrive at the expression for a small parameter of the theory:

$$\alpha = \frac{0.11 r_W}{a_0 Z^{1/3}} . \tag{3.19}$$

Table 9 contains the values of the Wigner–Seitz radius [19] for some clusters, the values of a small parameter α found in

Table 9. Parameters of ion braking in metal clusters.

	Cr	Cu	W	Hg
r_W, Å	1.41	1.47	1.60	1.80
α	0.16 (0.20)	0.17 (0.21)	0.18 (0.23)	0.21 (0.26)
$C(\alpha)$	0.87 (0.67)	0.83 (0.63)	0.77 (0.55)	0.66 (0.43)

accordance with formula (3.19), and also values of the factor $C(\alpha)$ in formula (3.14) for these clusters. Note that for the collision velocities under consideration the effective ion charge Z is in the range from 5 to 10. Table 9 gives the parameters for $Z = 10$, and the parameters at $Z = 5$ are given in parentheses.

The mean free path λ of an ion that transfers its kinetic energy to electrons of colliding clusters is defined as

$$\frac{\lambda}{a_0} = \frac{M}{m_e}\frac{\hbar v}{Ze^2}\frac{1}{C}, \tag{3.20}$$

where M is the atomic ion mass. Under typical conditions, the reduced length on which ions lose their energy is $\lambda/a_0 \sim 10^3 - 10^4$, thus exceeding the cluster size.

Note that within the framework of the model under consideration we assumed the electron subsystem as residing in the ground state. But this only takes place at the first stage of cluster collisions. Even upon mixing of two electron subsystems in the course of mutual penetration of two clusters, the electron subsystem is excited. This violates the assumption about a small portion of electrons partaking in transitions, and this very fact provides a small ion braking rate or a large ion mean free path with respect to ion kinetic energy transfer to electrons. Therefore, we consider another limiting case for the excitation of the electron subsystem by moving ions, assuming final electron states not to be occupied and electrons to be free in the course of ion scattering. Then, the rate of ion braking due to electron excitation is given by [142, 143]

$$-\frac{d\varepsilon}{dt} = N_e v \frac{4\pi Z e^4}{m_e v^2}\ln\Lambda. \tag{3.21}$$

Here, v is the ion velocity inside the electron subsystem, and ion scattering on different electrons proceeds independently; $\Lambda = p_{max}/p_{min}$, where $p_{max} = m_e v$ is the maximum momentum transferring to an electron, and the minimum transferred momentum p_{min} is determined by the structure of the electron subsystem. To make an estimate of the ion mean free path in electron medium, we take $\ln\Lambda \approx 5-10$ and use formula (3.18) for the number density of electrons. Then formula (3.21) gives

$$\lambda = \frac{\varepsilon m_e v^2 r_W^3}{3Z^2 e^4 \ln\Lambda}. \tag{3.22}$$

In the above limiting cases when an ion is moving inside an unexcited or excited electron subsystem, the ion mean free paths according to formulas (3.20) and (3.22) differ by several orders of magnitude. Therefore, these models give a coarse description of ion braking in cluster collisions.

Figure 8 illustrates the schematics of the collision of two cluster beams resulting in X-ray emission. Charged clusters from a cluster source are accelerated in an external electric field. We use as an estimate the maximum cluster charge [133] and typical number densities of bound atoms in intense cluster beams [134]. Then a typical cluster charge equals approximately $n^{1/2}e$, and the electric potential for acceleration of the cluster beam is taken to be $U = 1$ MV. Each cluster consists of $n \sim 10^6$ atoms, and its acquired energy is ~ 1 MeV per unit charge, or ~ 1 keV per nucleus. This corresponds to the relative velocity $v \approx 10^7$ cm s^{-1} of cluster collisions. Under these conditions, the mean free path for cluster ions

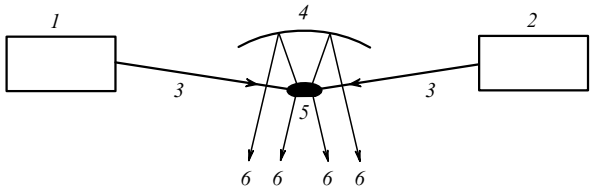

Figure 8. The character of the collision of two pulse cluster beams [136, 139]: *1*, *2* — pulse cluster beam generators, *3* — cluster beams, *4* — reflector, *5* — the region of intersection of cluster beams, and *6* — X-ray emission of cluster beams.

is, according to formula (3.20), $\lambda \sim 10^3 a_0$, and formula (3.22) gives $\lambda \ll a_0$. Hence, the optimal cluster size depends on the first stage of ion braking, which leads to initial excitation of the cluster electron subsystem. When the total kinetic energy of ions transfers to electron excitation energy, the electron subsystem will be heated to the effective temperature ~ 100 eV under these conditions.

Thus, cluster collisions lead to the formation of a plasma with a high temperature. This plasma is analogous to that resulting from irradiation of a cluster beam by an intense femtosecond laser pulse. The lifetime of a nonuniform plasma, i.e., joined clusters in the course of their collision, is $\sim r_W n^{1/3}/v \sim 10^{-13}$ s under the given collision parameters. Excited multicharge ions are also formed at this stage of system evolution, and subsequently they can emit X-ray photons. Based on the analogy to the processes proceeding in the laser case, one can expect the efficiency of transformation of the ion kinetic energy to the energy of X-rays to be the same as for the laser excitation method, i.e., $\sim 1\%$.

Assuming that the collision of two clusters leads to the conversion of cluster kinetic energy into the energy of electron excitation, we find the following typical times for this process. The lifetime of a joined cluster is $\sim 10^{-13}$ s and corresponds to the expansion time of a cluster excited by a laser pulse. The typical time of transformation of a nonuniform cluster plasma into a uniform plasma is $\sim 10^{-12} - 10^{-11}$ s, being identical in both cases, and the typical fly-off time of cluster beams in this case, or the time of expansion for a uniform plasma in the case of a laser irradiation, reaches $\sim 10^{-10}$ s. In addition, the electric potential of the beams of charged clusters is 10 – 100 kV for the collision of cluster beams, and is ~ 10 kV for the laser pulse. Thus, both cases of cluster excitation are characterized by processes of an identical nature, the same orders of magnitude for the parameters of these processes, and identical applications. The possibilities themselves for applications of these concepts depend on the experimental technique employed, and its development can give another character to the competition of these methods in the future.

It should be noted that the analysis of laser excitation of cluster beams is supported in large measure by experimental investigations, whereas experiments on the excitation of clusters as a result of the collision of cluster beams is practically absent. Our experience in analyzing the laser excitation of cluster beams shows that the character of processes constructed on the basis of simple models can differ from the real character. This is related first and foremost to the strong excitation of the cluster plasma, strong focusing of the laser signal, and high intensity of the focused laser pulse. Then, collective processes in the plasma become important due to the nonuniformity of the electro-

magnetic wave, the character of its modulation, etc. Therefore, simple models provide only a qualitative description of the character of plasma evolution. Nevertheless, a simple analysis shows that the method of creating electron excitations as a result of the collision of cluster beams has considerable promise, and forming a hot plasma in this manner is analogous to that resulting from the laser excitation of cluster beams.

4. Femtosecond cluster plasma as a generator of neutrons

4.1 Peculiarities of a fusion reaction involving deuterons

Neutrons can result from the collisions of fast heavy hydrogen isotopes — deuterium and tritium (see Fig. 9). The process of neutron formation in collisions of tritium nuclei is more effective but, because of tritium radioactivity, its usage requires the specific equipment and methods of refinement that makes this process practically inaccessible. Therefore, below we restrict ourselves to processes involving deuterons, where neutrons are formed according to the scheme

$$\mathrm{d} + \mathrm{d} \rightarrow {}^3\mathrm{He} + \mathrm{n}\,. \tag{4.1}$$

As a result of fusion reaction (4.1), the energy release amounts to 2.45 MeV per neutron, and this process is effective at collision energies up to hundreds of keV. The cross section of process (4.1) drops sharply at small energies [144], and in the range 20 – 200 keV in the laboratory frame of reference the fusion cross section is large, but it is not maximal. The measurement accuracy of the cross section of process (4.1) is about 10% [144] and is approximated by the dependence

$$\sigma_{\mathrm{fus}} = \frac{1.074 \times 10^5 + 330\varepsilon - 0.0635\varepsilon^2}{\varepsilon} \exp\left(-\frac{44.4}{\sqrt{\varepsilon}}\right) \tag{4.2}$$

in the above energy range with the accuracy indicated. The cross section σ_{fus} of fusion reaction (4.1) is given in mbarns (10^{-27} cm^2), and the deuteron energy ε in the laboratory frame of reference is expressed in keV. Note that in thermonuclear reactor containing a hot equilibrium (or almost equilibrium) plasma the fusion reaction is determined by the tail of the energy distribution function of deuterons. This allows one to realize in these reactors the Lawson criterion according to which the released energy of a fusion process is compensated for by the energy input into a plasma.

In the scheme under consideration, the fusion reaction proceeds in the course of relaxation when fast deuterium ions lose energy as a result of elastic collisions with target nuclei, and, until this energy is enough, they can partake in the fusion reaction with target nuclei. Because the cross section of ion

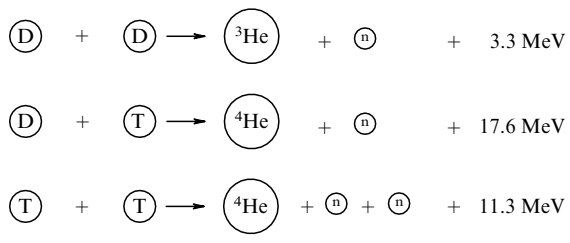

Figure 9. Fusion reactions involving deuterium and tritium nuclei.

elastic scattering significantly exceeds the cross section of the fusion reaction, the probability of a test deuteron partaking in the fusion reaction in the course of its braking is small. Moreover, this probability is so small that the Lawson criterion is not fulfilled in spite of the high energy released during the fusion reaction compared to the deuteron kinetic energy. This means that a thermonuclear reactor cannot be constructed on the basis of this scheme which admits only neutron generation. Nevertheless, this scheme of neutron generation by virtue of producing fast deuterium atoms or ions deserves attention because of the simplicity of the experimental technique employed and the availability of various versions. Below, we shall analyze this method of neutron generation.

Within the framework of this scheme, fast deuterium atoms and ions are directed to a target that contains deuterium and are braked in it. In the course of collisions with deuterium nuclei, a test fast deuteron can partake in fusion reaction (4.1), though the probability of this process is small and drops sharply with a decrease in deuteron energy. Deuteron braking in a deuterium-containing target proceeds as a result of two mechanisms of deuteron interaction with a target: excitation of a target electron subsystem, and elastic scattering of deuterons on target nuclei due to Coulomb interaction between them. If the first mechanism is possible, deuteron braking proceeds much faster, and the efficiency of neutron formation is lower if compared to the case when an inelastic process does not go. Being guided by a deuteron energy of dozens of keV, one can expect the absence of the inelastic channel in gaseous targets because the cross section of inelastic scattering in this case is relatively small. Moreover, inelastic collision processes are not essential for a plasma target because of a small exchange of energy between a colliding ion and free electron. But in the braking of an individual deuteron in a condensed (solid or liquid) target excitation of the target electron component may determine the loss of its energy. But if deuterons are constituents of a fast cluster penetrating to the target's interior, excitation of the electron subsystem of a target may be relatively small because the same target atom partakes in multiple collisions, and the energy transferred to one electron is restricted. Thus, there are many cases when the braking of a fast deuteron in a target is determined by its elastic collisions with target nuclei, and excitation of the target electron component is not essential.

Below, we consider just this case of fast deuteron braking as a result of elastic scattering on target nuclei [107, 145] that leads to a higher efficiency of neutron generation if compared with excitation of the target electron component. Because of the high energy of impinging deuteron, its scattering on target nuclei takes place upon their approach at small distances compared to atomic sizes. Hence, braking of individual, fast, cluster deuterons proceeds independently as a result of pair collisions with target nuclei, i.e., this process is analogous to that for gaseous targets. Then the braking rate, as well as the rate of fusion reaction (4.1), are proportional to the number density of target deuterons, and these processes result from pair collisions because the cross sections of these processes are small in comparison with atomic cross sections. Hence, the relative probabilities of the fusion process and energy loss are independent of the target density, and it is convenient to introduce as a characteristic of the fusion reaction in the course of deuteron braking the probability w_{fus} of a deuteron partaking in fusion reaction (4.1) in the course of deuteron

braking. This quantity is given by the formula [107, 145]

$$w_{\rm fus} = \int_0^{\varepsilon} N_{\rm i} v \sigma_{\rm fus} \frac{{\rm d}\varepsilon}{{\rm d}\varepsilon/{\rm d}t}\,, \tag{4.3}$$

where N is the number density of target deuterons, v is the velocity of a fast deuteron, and ${\rm d}\varepsilon/{\rm d}t$ is the rate of change of the deuteron energy.

A decrease in the fast deuteron energy as a result of the collision with a nuclei of charge Z is determined by the Rutherford formula (2.28) that at a small energy change $\Delta\varepsilon$ in the laboratory frame of reference, in comparison with an energy ε of a fast deuteron, is given by [21]

$${\rm d}\sigma = \frac{\pi Z^2 e^4}{\varepsilon(\Delta\varepsilon)^2}\,{\rm d}\Delta\varepsilon\,, \tag{4.4}$$

where the deuteron charge is unity. The braking of fast deuterons in a gas of nuclei of charge Z is determined by ion scattering with a small energy change. This gives the following expression for the rate of change of the deuteron energy ε in the course of its braking [21, 146]:

$$\frac{{\rm d}\varepsilon}{{\rm d}t} = \int(\varepsilon-\varepsilon')N_{\rm i} v\,{\rm d}\sigma\,(\varepsilon\to\varepsilon') = N_{\rm i} v\,\frac{\pi Z^4 e^4}{\varepsilon}\int\frac{{\rm d}\Delta\varepsilon}{\Delta\varepsilon}$$
$$= N_{\rm i} v\,\frac{\pi Z^2 e^4}{\varepsilon}\ln\left(\frac{\Delta\varepsilon_{\max}}{\Delta\varepsilon_{\min}}\right), \tag{4.5}$$

where $N_{\rm i}$ is the number density of target nuclei, v is the velocity of a fast deuteron, ε, ε' are the energies of a fast deuteron before and after collision in the laboratory system of coordinates, and the energy change $\Delta\varepsilon = \varepsilon - \varepsilon'$ for a fast deuteron is relatively small. Evidently, the maximum energy change is $\Delta\varepsilon_{\max} \sim \varepsilon$, and the minimum energy change for a fast deuteron corresponds to the impact parameter of the collision, which is on the order of the distance between nearest neighbors (about an atomic size a_0). Therefore, the minimum energy change is equal by an order of magnitude to

$$\Delta\varepsilon_{\min} = \frac{Z^2 e^2}{\varepsilon a_0}\,.$$

From this follows the expression for the Coulomb logarithm:

$$\ln\Lambda = 2\ln\left(\frac{\varepsilon}{Ze^2/a_0}\right).$$

In particular, at the deuteron energy $\varepsilon = 100$ keV the minimum energy that is transferred to motionless deuterons of a target is $\varepsilon_{\min} \sim 3\times10^{-4}$ eV, corresponding to the Coulomb logarithm $\ln\Lambda \approx 15$. We shall use this value of the Coulomb logarithm in subsequent estimations.

Substituting formula (4.4) into (4.3), for the probability of neutron generation as a result of deuteron braking from the initial energy ε_0 in a deuterium-containing medium with target nuclei of charge Z we find the following expression:

$$w_{\rm fus}(\varepsilon_0) = \int_0^{\varepsilon_0} \frac{\sigma_{\rm fus}(\varepsilon)\varepsilon\,{\rm d}\varepsilon}{\pi Z^2 e^4 \ln\Lambda}\,. \tag{4.6}$$

This formula is generalized in a simple manner to the case where a target contains nuclei of different charges, since deuteron scattering on these nuclei proceeds independently. Indeed, if the target contains several components and the concentration of nuclei of the ith component is c_i and the nuclear charge for this component is Z_i, the probability $w_{\rm fus}(\varepsilon_0)$ of partaking a deuteron in a fusion reaction in the deuterium target is multiplied by the quantity $c_{\rm D}\left(\sum_i c_i Z_i^2\right)^{-1}$, where $c_{\rm D}$ is the concentration of deuterium nuclei. In particular, if a target contains molecules CD_4 or D_2O, this factor corresponds to a decrease in the fusion reaction probability $w_{\rm fus}(\varepsilon_0)$ by 10 and 33 times, respectively, in comparison with the deuterium target.

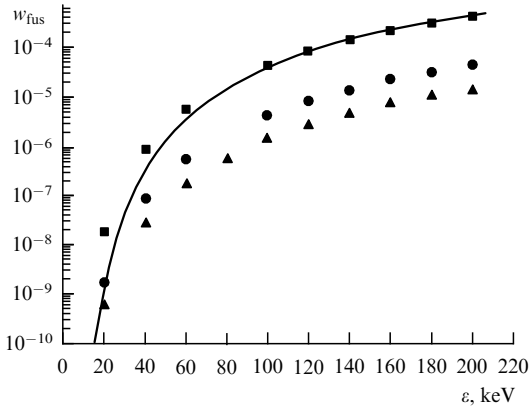

Figure 10. The probability of neutron generation in the course of braking of a fast deuteron in a deuterium-containing matter, calculated according to formula (4.6) for the following targets: D_2 (■), CD_4 (●), D_2O (▲). Solid curve is the approximation (4.7) for a deuterium target.

Figure 10 depicts the dependences $w_{\rm fus}(\varepsilon_0)$ of the neutron generation probability on the initial deuteron energy as a result of the braking of a fast deuteron in deuterium-containing matter. These dependences were calculated on the basis of formula (4.6) for three targets. Because of the sharp dependence of the fusion reaction cross section on energy, it is convenient to approximate the probability $w_{\rm fus}(\varepsilon)$ by the dependence

$$w_{\rm fus}(\varepsilon_0) = C\exp\left(-\sqrt{\frac{\varepsilon_0}{\varepsilon}}\right), \tag{4.7}$$

and the following parameters are appropriate to the deuterium target: $C = 0.18$, and $\varepsilon_0 = 7$ MeV in the collision energy range $\varepsilon = 20-200$ keV. From Fig. 10 it follows that this approximation is not correct at small deuteron energies.

If we account for the sharp dependence of the fusion cross section (4.2) on the energy of a fast deuteron, we can reduce formula (4.6) to the form [145]

$$w_{\rm fus} = \frac{\sigma_{\rm fus}(\varepsilon)\varepsilon}{32\pi e^4 \ln\Lambda}\left(\frac{{\rm d}\ln\sigma_{\rm fus}}{{\rm d}\varepsilon}\right)^{-1}. \tag{4.8}$$

Table 10 gives the values of this quantity together with the cross section of fusion process (4.2), which were obtained on

Table 10. Parameters of the fusion reaction and fast deuteron braking in condensed deuterium.

ε, keV	$\sigma_{\rm fus}$, mb	$\frac{{\rm d}\ln\sigma_{\rm fus}}{{\rm d}\varepsilon}$, 0.01 keV^{-1}	$w_{\rm fus}$, 10^{-6}
20	0.278	22	0.063
40	2.69	7.6	0.36
60	6.86	4.2	1.0
80	11.6	2.7	2.0
100	16.5	2.0	3.8
120	21.2	1.5	5.6
140	25.5	1.2	8.1
160	29.6	1.0	11

Table 11. Values of $w_{\text{fus}}(T)$ for various targets.

T, keV	D_2	CD_4	D_2O
5	2.5×10^{-9}	2.5×10^{-10}	7.6×10^{-11}
10	1.3×10^{-7}	1.3×10^{-8}	3.9×10^{-9}
15	9.4×10^{-7}	9.4×10^{-8}	2.9×10^{-8}
20	3.3×10^{-6}	3.3×10^{-7}	1.0×10^{-7}
30	1.6×10^{-5}	1.6×10^{-6}	4.8×10^{-7}
40	4.2×10^{-5}	4.2×10^{-6}	1.3×10^{-6}
50	8.4×10^{-5}	8.4×10^{-6}	2.5×10^{-6}
60	1.4×10^{-4}	1.4×10^{-5}	4.3×10^{-6}

the basis of data from Ref. [144]. In this table there are also the values of $w_{\text{fus}}(\varepsilon_0)$ for the deuterium target.

Because of the sharp dependence of the fusion cross section (4.2) on the energy of a fast deuteron, the efficiency of neutron generation is determined by the tail of the energy distribution function of fast deuterons, which may be approximated by the Maxwell distribution function $f(\varepsilon)$. Then, the probability of a fusion reaction is given by

$$w_{\text{fus}}(T) = \int_0^\infty w_{\text{fus}}(\varepsilon) f(\varepsilon) \, \mathrm{d}\varepsilon \,. \tag{4.9}$$

Table 11 contains the values of $w_{\text{fus}}(T)$ in an appropriate range of temperatures.

Note that according to the above results, the higher the initial energy of a fast deuteron, the higher the probability of the fusion reaction. But in reality, the fast deuteron energy is bounded from above because the mean free path of a fast deuteron is proportional to the square of the initial energy. Therefore, at large energies a fast deuteron can go outside a region occupied by a deuterium-containing target.

Let us determine the deuteron mean free path λ in a deuterium target, i.e., the distance which is passed by a deuteron up to its stopping. In accordance with the above formulas for deuteron slowing down, the deuteron mean free path is determined by its initial energy and is given by

$$N_{\text{i}} \lambda = \frac{\varepsilon^2}{32\pi e^4 \ln \Lambda} \,, \tag{4.10}$$

where ε is the initial deuteron energy, and N_{i} is the number density of target nuclei. Because of the high energy of a fast deuteron, its scattering occurs on coming within short distances to a scattering nucleus in comparison with the distance between nearest nuclei. Hence, matter that scatters deuterons behaves as a gas for fast deuterons, and their braking does not depend on its aggregate state. Let us also introduce the mean free path of deuterons λ_{fus} on which the fusion reaction basically proceeds, and this is given by the formula

$$N_{\text{i}} \lambda_{\text{fus}} = \int_0^{\varepsilon_0} \frac{\varepsilon w_{\text{fus}}(\varepsilon) \, \mathrm{d}\varepsilon}{16\pi e^4 \ln \Lambda \, w_{\text{fus}}(\varepsilon_0)} \,. \tag{4.11}$$

Table 12 contains reduced values of the mean free path of deuterons in a deuterium target (N_{i} is the number density of target nuclei, λ is the mean free path of fast deuterons due to elastic scattering, and λ_{fus} is the deuteron mean free path with respect to the fusion reaction). Table 12 also gives the mean free path λ_{s} of a fast deuteron in solid deuterium that has the density of 0.169 g cm^{-3}. Evidently, the target size must exceed the deuteron mean free path in the appropriate medium, and

Table 12. Reduced values of the deuteron mean free path in a deuterium target and in solid deuterium.

ε, keV	$N_{\text{i}}\lambda$, 10^{20} cm^{-2}	$N_{\text{i}}\lambda_{\text{fus}}$, 10^{20} cm^{-2}	λ_{s}, 10^{-3} cm
20	0.28	0.047	0.60
40	1.1	0.24	2.4
60	2.5	0.63	5.4
80	4.4	1.2	9.5
100	6.9	2.1	15
120	9.9	3.2	21
140	13	4.6	29
160	18	6.3	38
180	22	8.2	48
200	28	10	60

this fact may be of importance in choosing the target. The passage from a deuterium target to other deuterium-containing targets leads to a decrease in the reduced mean free path of deuterons by $c_{\text{D}} \left(\sum_i c_i Z_i^2 \right)^{-1}$ times, where c_i is the concentration of the ith component, and Z_i is its nuclear charge. For targets consisting of molecules CD_4 and D_2O, this factor is 10 and 33, respectively.

The above analysis demonstrates the possibility of creating a neutron source driven by the pulse excitation of a deuterium-containing target. The efficiency of neutron generation in the course of relaxation of fast deuterons is the greater, the higher is the initial deuteron energy. But the probability of the fusion reaction is always small, i.e., the Lawson criterion is not fulfilled in this excitation scheme. Therefore, the pulse systems under consideration may be used as neutron sources only.

4.2 The fusion process as a result of laser irradiation of a cluster beam

Excitation of a beam of deuterium clusters by a short laser pulse can be employed for creating a compact source of neutrons [65–67, 147–149]. Then, the evolution of a cluster plasma develops analogously to the case when it is used as an X-ray source. Indeed, after irradiation of a deuterium cluster beam by a laser pulse, electrons leave the cluster, and a high electric potential of a remaining ion system compels the cluster to expand due to a noncompensated charge. The highest electric potential is created on the cluster surface and, correspondingly, ions located near the cluster surface acquire the maximum energy and can partake in the fusion reaction after the decay of the cluster plasma. Of course, this scheme simplifies the real situation, and experimental studies allow one to exhibit the detailed character of the evolution of a cluster plasma taking into account additional processes. Restricted by the qualitative description of processes which accompany the generation of neutrons, below we shall portray the simplest character of the evolution of a deuterium cluster plasma.

The energy of ions which are located at the beginning on the surface of a cluster is determined after its expansion by the surface electric potential and can reach dozens of keV. Subsequent collisions of fast deuterium ions after cluster decay, when the plasma becomes uniform, can lead to a fusion reaction involving such ions. This scheme of neutron generation cannot serve as a basis for a thermonuclear reactor, because the Lawson criterion is lower by four–five orders of magnitude than in the case of a self-maintaining fusion reaction. Table 13 lists the parameters of some experiments with neutron generation as a result of cluster

Table 13. Parameters of a laser-driven fusion reaction for a cluster target.

Target	E, J	I, W cm^{-2}	τ, fs	n	$T_{\rm eff}$, keV	Ref.
D_2	0.12	2×10^{16}	35	1×10^4	6	[147]
D_2	10	2×10^{20}	100	2×10^6	7	[150]
CD_4	0.8	2×10^{17}	35	7×10^3	6	[67]
CD_4	2.5	4×10^{19}	100	1×10^5	8	[154]
D_2O	0.6	12×10^{19}	35	6×10^3	8	[151]

Note. The chemical composition of clusters is specified in the column 'target'. I is the intensity of the laser pulse of a wavelength of about 0.8 μm, E and τ are the pulse energy and duration, respectively, n is the number of generated neutrons per pulse, and $T_{\rm eff}$ is the effective temperature of fast deuterons.

irradiation by a high-power laser pulse. According to this table, laser irradiation of deuterium or deuterium-containing cluster beams leads to a fusion reaction with generation of neutrons. The effective temperature $T_{\rm eff}$ of an accelerated deuteron bunch relates to the assumption of the Maxwell distribution for fast deuterons which are responsible for neutron generation, and the probability of this process is given in Table 11.

In neutron generation with a laser-irradiated deuterium cluster beam, complete ionization of clusters proceeds firstly with a loss of all the electrons, and then fast deuterons resulting from cluster decay partake in a fusion reaction at the stage when the plasma becomes uniform. This simple model allows one to find the dependence of the neutron yield on the process parameters, in particular, on the cluster size in the beam [138]. For the most part, this model is in accord with the experimental neutron yield [154] and shows that the basic parameter of this process is the ratio of time of cluster ionization as a whole to time of cluster expansion. From this model it follows that ions located on the cluster surface after its total ionization have the kinetic energy eQ/R after cluster decay, where $Q \sim R^3$ is the charge, and R is the cluster radius. This gives that the efficiency of neutron generation increases with an increase in cluster size. But for this it is necessary to ionize such a cluster, and there appears an optimal cluster size for neutron generation at a given laser intensity. This relates especially to carbon – deuterium clusters which are created more simply than deuterium clusters because of a higher boiling point. In this case, however, a partial carbon ionization proceeds along with deuterium ionization that shifts the parameters of optimal conditions.

Nevertheless, the basic process for neutron generation is a release of cluster electrons that leads to a cluster charging and creates a high electric potential for ions on the cluster surface. This potential energy of ions is transformed subsequently to their kinetic energy that is utilized in the fusion reaction. But the same chain of processes accompanies irradiation of the deuterium surface by a laser pulse, which can also lead to neutron generation. Moreover, according to experimental investigations, this case gives a higher yield of neutrons for a carbon – deuterium target that amounts to 10^7 neutrons per pulse [152, 153]. This also results from the possibility of using longer pulses for irradiating a solid target.

Energy distributions of protons resulting from a decay of hydrogen clusters excited by a femtosecond laser pulse of intensity 6×10^{16} W cm^{-2} were measured in experiment [107] where the average proton energy was 8.1 keV. The observed proton spectrum accords well with the calculated results for a simple model of a uniform spherical cluster. The maximum proton energy is determined by both the cluster size and the laser intensity.

Experimental studies [68, 154] of the explosion of deuterium clusters by superintense laser pulses of 100 TW show the sensitivity of the ion energy and neutron yield to the duration of the laser pulse. These quantities are determined by the ratio of total ionization time for a cluster to its expansion time. A decrease in the pulse duration from 1 ps to 100 fs leads to an increase in the neutron yield by approximately 10 times. This finding is independent of the laser pulse energy over a range from 0.1 to 10 J.

Similar investigations of energy distributions of protons under irradiation of hydrogen clusters by intense laser pulses (the intensity was 10^{16} W cm^{-2}, and the pulse duration was 65 fs) in experiment [114] revealed the linear dependence of maximum and average proton energies on the square of the cluster radius. This proves the Coulomb mechanism of cluster explosion, and this mechanism dominates for small clusters with a radius below 20 Å. Inner ionization of clusters then has an over-barrier character.

The above model of cluster processes at neutron generation, when cluster ions acquire energy as a result of the decay of a charged cluster, is, of course, simplified and crude, which is confirmed by experimental studies. In particular, measurement of the angular distribution of neutrons for irradiated D_2 and CD_4 clusters [155, 157] shows a small anisotropy in the escape directions of neutrons. This inference confirms the complex character of laser-excited cluster plasma and the fact that its evolution does not follow simple models. Such a conclusion also follows from the sensitivity of neutron yield to the laser pulse shape at a radiation power of 10^{14} W [68].

An anisotropy in the explosion of hydrogen clusters was observed for intense laser pulses with a duration from 40 to 200 fs [156]. As opposed to the above simple model, the primary yield of fast protons proceeds in the polarization direction of a laser wave, which is explained by vacuum electron heating (the Brunel mechanism). Similar results were obtained from the irradiation of clusters consisting of a mixture of light (deuterium) and heavy atoms by an intense femtosecond laser pulse [102]. The heavy atoms intensify the cluster Coulomb explosion and increase the probability of a fusion reaction involving deuterium nuclei. This was confirmed experimentally for clusters consisting of a mixture of deuterium and methane.

Angular distributions of neutrons resulting from Coulomb explosion of deuterium clusters (and clusters of CD_4 molecules) under the action of terawatt laser pulses with a duration of 40 fs exhibit a small anisotropy in the neutron yield [157]. This was explained by an anisotropy in the differential cross section for a fusion reaction of two deuterons with neutron and ^{3}He nucleus formation.

The angular anisotropy of formed neutrons testifies to the complex character of processes accompanying neutron generation as a result of the interaction of cluster beams with a laser pulse. Since the neutron yield is determined by fast deuterium ions, mechanisms of their acceleration are of importance and can include, according to experiments, both collective phenomena and specific effects of interaction between atomic systems and a strong electromagnetic wave. Along with the laser intensity, these processes depend on the target size, because processes that are responsible for neutron generation take place on or near the surface of large clusters.

The specific character of laser pulse action on a cluster beam follows from experiments with very large clusters and drops containing deuterium. In particular, experiments exploring the evolution of heavy water drops of diameter 20 μm excited by a laser pulse of duration 40 fs and intensity up to 10^{19} W cm^{-2} [158] revealed that the neutrons formed escape primarily in the direction of propagation of the laser wave. The total neutron yield is lower than that for deuterium clusters and is on average 1200 neutrons per pulse. A drop decrease of up to 150 nm leads to a yield increase of up to 6×10^3 neutrons per pulse [159]. In addition, the specific character of the spectrum of high-energy deuterium ions with energy up to 1 MeV that is characterized by dips testifies to the essential role of collective processes in the cluster plasma evolution. Measurements of neutron spectra in the irradiation of heavy water drops by a laser pulse of intensity 3×10^{19} W cm^{-2} [160] point to two mechanisms of acceleration of deuterium ions: due to a ponderomotive force from the laser wave, and because of the nonuniformity of the electromagnetic field near the laser beam focus.

On the basis of a study of the fusion reaction involving deuterons [160] using microdrops of heavy water and femtosecond laser pulses of intensity 3×10^{19} W cm^{-2}, the mechanism of deuteron heating was suggested when acceleration of electrons under the action of the ponderomotive force up to MeV energies at the first stage of the pulse passage creates a capacitor, so that deuterons moving behind the electrons are accelerated by the field of this capacitor up to similar energies at the second stage of this process.

The explosion of individual microdrops of heavy water 0.2 mm in diameter under irradiation by a laser pulse of duration 40 fs and maximum intensity 10^{19} W cm^{-2} within the framework of experiment [160] gave 1200 neutrons per pulse. This small amount of neutrons was explained by their isotropic formation in the drop explosion. A drop size decrease to 150 nm leads to an increase in the neutron yield of up to 6300 neutrons per pulse, which is explained by the directional motion of deuterons.

Note that the above scheme of deuteron acceleration as a result of irradiation of a cluster beam by a laser pulse, which consists in cluster ionization at the first stage and subsequent decay of a charged cluster with the acceleration of surface layers under the action of the cluster electric potential, can be a basis for understanding the character of the deuteron acceleration process. Subsequently including in this scheme collective processes and the specific effects of cluster interaction with a strong electromagnetic wave creates a variety of acceleration regimes under laser irradiation involving both a cluster beam and a solid surface. Below, we shall give some mechanisms of this interaction that follow from experimental studies and computer simulations.

Theoretical analysis [161] of fusion reactions resulting from Coulomb explosion of fully ionized $(NH_3)_n$ and $(CH_4)_n$ clusters showed that these reactions take place due to collisions of protons with carbon, nitrogen, and oxygen nuclei. Similar reactions in hot stars generate fusion energy. All the electrons leave clusters with radii ranging from 30 to 70 nm at an intensity of femtosecond laser radiation above 10^{19} W cm^{-2}, and the protons formed have an energy of about 3 MeV, while the energy of heavy nuclei can reach 30 MeV. Similar computer simulation [162] by the method of molecular dynamics of these processes for a number of deuterium molecules in a cluster ranging from 250 up to several million, an intensity of laser pulses of $10^{15} - 10^{18}$ W cm^{-2}, and pulse duration between 25 and 50 fs revealed strong laser absorption in a thin skin layer for large clusters consisting of about 5×10^6 molecules or having a radius of 330 Å.

The analysis of neutron generation and laser-driven deuteron acceleration [163] testifies to the nearby energies of accelerated deuterons with a dispersion of the kinetic energies of about 2 MeV. This quasienergetic peak was observed in the irradiation of heavy water microdrops by laser pulses with a duration of 40 fs and peak intensity of 10^{19} W cm^{-2}. This behavior is explained by spatial separation of deuterons and oxygen nuclei in the course of acceleration.

Studies of neutron generation resulting from the excitation of a beam of deuterium-containing clusters by a laser pulse help in understanding the character of cluster excitation and the evolution of a cluster plasma in the process of fast deuteron generation. Fast deuterons result from Coulomb explosion of a charged cluster, which can be accompanied by a variety of collective processes involving charged particles and their interaction with a strong electromagnetic field in a plasma.

4.3 Neutron generation in collisions of deuterium cluster beams

Collisions between fast deuterium atoms or ions with an energy of the order of 100 keV and deuterium matter lead to neutron generation (see Table 12). A target may be a deuterium cluster, a droplet, a particle, or deuterium film. For any target, neutrons are generated in the course of braking of the deuterons which are scattered elastically on target nuclei, and the excitation of the electron subsystem in the braking process is assumed to be weak, leading to a relatively large mean free path of a deuterium ion in a target (see Table 12). This influences the scheme of a neutron generator under consideration, where a beam of accelerated deuterium clusters encounters a target, and the fusion reaction can proceed as long as the deuterons do not lose their energy.

In determining the target parameters, we assume the number density of deuterium atoms to be identical for different targets because its atomic structure is primarily determined by the interaction of nearest neighbors. It is close for solid deuterium and hydrogen, and taking the solid hydrogen density as 0.076 g cm^{-3} according to Ref. [164], we obtain the number density $N_0 = 4.6 \times 10^{22}$ cm^{-3} of hydrogen atoms in solid hydrogen, and we take the same value for the number density of deuterium atoms in solid deuterium. Correspondingly, the Wigner–Seitz radius for a deuterium cluster is $r_W = 1.7$ Å, and Table 12 contains the mean free paths of fast deuterons in a deuterium target.

Note that the character of the fusion process is identical for the braking of both fast deuterium ions and deuterium clusters. Hence, the advantage of using clusters consists in the possibility of adjusting the cluster parameters to parameters of an energy source for their acceleration. In considering the scheme of generation of fast deuterium clusters, we take the energy of an individual deuteron to be 100 keV, which corresponds to the velocity $v_d = 2.4 \times 10^8$ cm s^{-1} for fast deuterons and their clusters. For comparison, the speed of sound for deuterium at room temperature is on the order of 10^5 cm s^{-1}. Being guided by a pulse source [165] of the electric field, we take the potential of the electric field to be $U = 3$ MV, and the electric field strength to be $F = 10^6$ V cm^{-1}. This corresponds to a distance $L = 3$ cm

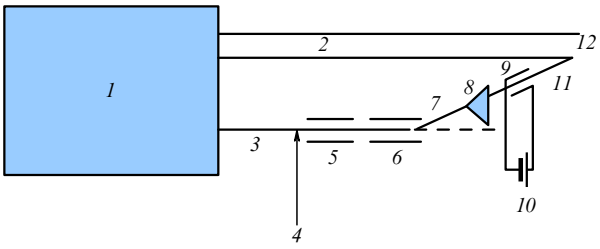

Figure 11. Schematics of neutron generation in the collision of two deuterium cluster beams: *1* — container with gaseous deuterium for the generation of cluster beams; *2* — wide beam of slow deuterium clusters; *3* — narrow beam of deuterium clusters; *4* — electron beam for ionization of xenon clusters; *5* — collector for electrons; *6* — weak electric field for the deflection of charged clusters; *7* — beam of charged clusters; *8* — skimmer; *9* — gap for the acceleration of charged clusters; *10* — source of a strong electric field; *11* — accelerated beam of charged clusters; *12* — region of fusion reaction, where accelerated clusters collide with a dense beam of slow large clusters.

between the plates of this generator. Clusters are accelerated in the space between these plates, and a typical time of acceleration equals $t \approx 20$ ns, corresponding to the typical duration of pulse voltage in accordance with the parameters of this electric field source [165]. In addition, the power of this source is relatively small.

An accelerated beam of deuterium clusters is directed at a target that comprises a dense cluster beam (Fig. 11), deuterium drop, or deuterium film where the fusion process (4.1) proceeds. Preliminarily, the clusters of a cluster beam are charged by a crossed electron beam with given parameters [134]. This standard scheme allows preparing the cluster beam of a given size and charge for acceleration [134]. In this case, in order to attain the energy 100 keV per deuteron at a voltage of $U = 3$ MV between accelerating plates it is necessary that a singly charged cluster consist of 30 deuterium atoms or 15 deuterium molecules. One can obtain clusters of this size by using a nozzle of a small size and the preliminary acceleration of a deuterium gas [166].

The number density of clusters being accelerated follows from the condition that the electric field strength due to an uncompensated charge of clusters is less than the electric field strength of the source. According to Poisson equation we have the following relation between the number density $N_{\rm cl}$ of elementary charges in the accelerating gap and the electric field strength F due to these charges:

$$N_{\rm cl} = \frac{F}{2\pi e L}\,, \tag{4.12}$$

where $F = 10^6$ V cm^{-1} is the electric field strength for an accelerating gap. From this we obtain the number density $N_{\rm cl} \sim 2 \times 10^{11}$ cm^{-3} of accelerated clusters, which corresponds to the number density $N_{\rm d} \sim 1 \times 10^{13}$ cm^{-3} of deuterons being accelerated. Note that a decrease in the distance between plates of the electric field source leads to an increase in the ultimate number density of charged clusters but conserves the total number of clusters at a given cross section of the gap. In particular, taking an accelerating gap in the form of a cylinder with a radius $r = 1$ mm, we obtain the total number of accelerated deuterons $n \sim 10^{12}$ (their weight is on the order of 0.3 ng). For acceleration of these deuterons, an electric energy of 3 mJ is required, which corresponds to the power of the pulse of 200 kW for deuteron acceleration. At the deuteron energy $\varepsilon = 100$ keV, this leads to the generation of 10^6 neutrons per pulse. Though this is an exaggerated estimate because we based it on the limiting values of the parameters, it gives appropriate scales of parameters for this method of neutron generation.

Let a target be a dense beam of deuterium clusters (see Fig. 11) and the number density of bound deuterons in this beam we take in accordance with experiment [137, 138] to be 5×10^{19} cm^{-3}. Then, at a beam energy of 100 keV per deuteron we obtain the mean free path of a fast deuteron in a dense cluster beam as 7 cm, as follows from the data in Table 10. As is seen, a dense cluster beam may be used as a target in the case of a small angle between colliding beams. Note that the indicated mean free path relates to the full braking of deuterons, while the main contribution to neutron generation is given by small changes in the initial deuteron energy, i.e., the mean free path with respect to neutron generation is markedly smaller. In particular, at the initial deuteron energy of 100 keV one half of the neutrons are formed at distances less than 3 cm. In addition, for a cluster target with the average number of deuterons $n = 3 \times 10^4$ per cluster that is used in experiments [148, 68], the mean free path of an accelerated cluster in the cluster matter is 7 μm (the cluster radius $R = 5.4$ nm corresponds to the collision cross section $\sigma = 9 \times 10^{-13}$ cm^2).

Let us consider the following aspect of deuteron braking. When a small deuterium cluster encounters a large cluster and passes through it, this cluster is divided into individual deuterons that are scattered inside the cluster independently. Therefore, the character of the braking process is identical for deuterium clusters and for individual deuterium ions, and the natural question arises of why the cluster beam is better for this problem than the beam of deuterium ions. We give three peculiarities of such a comparison. First, the pulse energy source has a certain electric voltage (in this case 3 MV), and this voltage must be transformed for the acceleration of ions. In the cluster case, optimal conditions are chosen by the cluster size. Second, the ultimate charge of beams that is identical in both cases results in an identical ultimate charge density, but the number of deuterons for a cluster beam is more than that for the deuterium ion beam. Third, the lifetime of the charged cluster beam due to its expansion under the action of the internal electric field is more in the case of the cluster beam compared to atomic ions possessing smaller masses. All these factors make the cluster method more attractive for neutron generation.

The neutron yield under the collision of cluster beams is comparable to that for the laser method of excitation of a cluster beam, where according to experiments [148, 68] a laser pulse of intensity 2×10^{20} W cm^{-2}, wavelength 800 nm, and pulse duration ranging from 100 fs to 1 ps, yielded 10^6 neutrons per pulse and an average deuteron energy of about 10 keV with an average cluster radius of about 5 nm (3×10^4 deuterons per cluster). Neutron formation was observed for 1.5 ns after the laser pulse cessation, and the maximum rate of neutron formation corresponded to 0.7 ns after the end of the laser pulse [66]. Note that the doubling time for the cluster radius due to its expansion was 20 fs [65] — that is, the fusion reaction took place primarily in a uniform plasma. A typical time of expansion of this plasma to the surrounding space was on the order of 1 ns.

This analysis shows that contemporary pulse generators of high voltage provide neutron generation in collisions of

cluster beams if one of these is accelerated in an external pulse electric field. This method is analogous to the laser method of cluster excitation for neutron generation. In the cluster method, however, the energy of a laser pulse is used for neutron generation, while in the method of collision of cluster beams the kinetic energy of accelerated deuterium clusters is used for the same purpose. These two methods are based on different experimental techniques and, therefore, they are alternatives. The competition between these methods will be determined by the development of corresponding experimental techniques.

5. Conclusions

A new experimental technique allows developing new methods in the research of atomic matter. Previous generations of physicists could not even think about a laboratory device that creates an electric field stronger than the atomic ones. New concepts are required for understanding the character of interaction of such fields with matter, and this is the content of contemporary physics that is based on a new experimental technique and new physical concepts.

Of course, analogs of contemporary experimental techniques have existed a long time. In particular, Van de Graaf generators created in the 1930s are analogs for the above-mentioned pulse sources that allow one to obtain megavolt voltages. But these pulse voltage sources [165] are based on other principles and, working in the prebreakdown regime, they constitute pulse nanosecond and picosecond devices. As a result, they are small compared to stationary installations and have a low power. At the same time, they are more effective and demand specific applications, like the above problem of neutron generation.

New experimental technique stimulates developing new applications. Comparing the above femtosecond high-power lasers for the generation of X-rays and neutrons, we note that standard sources of X-rays, based on collisions of electrons with an energy of dozens of keV with solids, are cheaper and more attractive for many medical applications. Nevertheless, the above-considered methods allow one to create more effective X-ray sources and with other spectral parameters. Indeed, X-ray emission in standard sources results from radiative transitions between discrete states involving inner atomic shells and their spectrum consists of some discriminatory lines. The radiation spectrum of the above systems results from emission of a hot plasma that gives a wider spectrum. It depends on a buffer gas, so that both this fact and a higher efficiency of energy transformation determine possible applications for such devices.

Thus, the development of an experimental technique is the locomotive that allows one to investigate new properties of atomic matter and leads to new applications. In this context clusters as a new physical object have become convenient for creating new energy sources. In its very essence, the above experimental technique allows the extreme excitation of matter when the input energy is restricted. At these scales of energy deposition, the clusters with their small enough atomic sizes are suitable objects.

Note one more peculiarity of the above experimental technique. In order to reach high yield parameters, it is necessary to utilize materials which work under extreme conditions. This requires specific materials, but these materials can hold up a restricted number of pulses. This means that such a technique is expensive not only in the production, but also in its exploitation. Therefore, in particular, the existing laser installations in Table 1, which allow one to create superatomic fields, are only found in highly developed countries. In the future these countries will have new technology, and a high pay for a new experimental technique is a pay for a future technology. In particular, these countries will have new lithography technology for the production of elements of micro- and nanoelectronics. Unfortunately, the attitude toward science in Russia does not allow creating the installations collected in Table 1, and this situation excludes Russia from the list of highly developed countries in years to come.

This paper is supported partially by RFBR grants Nos 06-02-16146-a and 07-02-00080a.

References

1. Ditmire T et al. *Phys. Rev. A* **53** 3379 (1996)
2. Ditmire T et al. *J. Phys. B: At. Mol. Opt. Phys.* **31** 2825 (1998)
3. Miura E et al. *Appl. Phys. B* **70** 783 (2000)
4. Stenz C et al. *Kvantovaya Elektron.* **30** 721 (2000) [*Quantum. Electron.* **30** 721 (2000)]
5. Junkel-Vives G C et al. *Phys. Rev. A* **64** 021201 (2001)
6. Mori M et al. *J. Appl. Phys.* **90** 3595 (2001)
7. Skobelev I Yu et al. *Zh. Eksp. Teor. Fiz.* **121** 1124 (2002) [*JETP* **94** 966 (2002)]
8. Ter-Avetisyan S et al. *Phys. Rev. E* **64** 036404 (2001)
9. Schnürer M et al. *Eur. Phys. J. D* **14** 331 (2001)
10. Krainov V P, Smirnov M B *Usp. Fiz. Nauk* **170** 969 (2000) [*Phys. Usp.* **43** 901 (2000)]
11. Krainov V P, Smirnov M B *Phys. Rep.* **370** 237 (2002)
12. Rühl E *Int. J. Mass Spectrom.* **229** 117 (2003)
13. Saalmann U, Siedschlag Ch, Rost J M *J. Phys. B: At. Mol. Opt. Phys.* **39** R39 (2006)
14. Keldysh L V *Zh. Eksp. Teor. Fiz.* **47** 1945 (1964) [*Sov. Phys. JETP* **20** 1307 (1965)]
15. Delone N B, Krainov V P *Multiphoton Processes in Atoms* 2nd ed. (Berlin: Springer-Verlag, 2000)
16. Bethe H A, Salpeter E E *Quantum Mechanics of One- and Two-Electron Atoms* (Berlin: Springer, 1957)
17. Cowan R D *The Theory of Atomic Structure and Spectra* (Berkeley: Univ. of California Press, 1981)
18. Smirnov M B, Krainov V P *Phys. Rev. A* **69** 043201 (2004)
19. Smirnov B M *Clusters and Small Particles: in Gases and Plasmas* (New York: Springer, 2000)
20. Smirnov M B, Becker W *Phys. Rev. A* **69** 013201 (2004)
21. Landau L D, Lifshitz E M *Mekhanika* (Mechanics) (Moscow: Nauka, 1973) [Translated into English (Oxford: Pergamon Press, 1975)]
22. Smirnov M B, Becker W *Phys. Rev. A* **74** 013201 (2006)
23. Kumarappan V, Kim K Y, Milchberg H M *Phys. Rev. Lett.* **94** 205004 (2005)
24. Saalmann U, Rost J-M *Phys. Rev. Lett.* **91** 223401 (2003)
25. Taguchi T, Antonsen T M (Jr.), Milchberg H M *Phys. Rev. Lett.* **92** 205003 (2004)
26. Döppner T et al. *Phys. Rev. Lett.* **94** 013401 (2005)
27. Liu J et al. *Phys. Rev. A* **73** 033201 (2006)
28. Sumeruk H A et al. *Phys. Rev. Lett.* **98** 045001 (2007)
29. Belkacem M et al. *Phys. Rev. A* **73** 051201(R) (2006)
30. Mulser P, Kanapathipillai M, Hoffmann D H H *Phys. Rev. Lett.* **95** 103401 (2005)
31. Mulser P, Kanapathipillai M *Phys. Rev. A* **71** 063201 (2005)
32. Fomichev S V et al. *J. Phys. B: At. Mol. Opt. Phys.* **36** 3817 (2003)
33. Fomichev S V et al. *Phys. Rev. A* **71** 013201 (2005)
34. Popruzhenko S V, Zaretsky D F, Becker W *J. Phys. B: At. Mol. Opt. Phys.* **39** 4933 (2006)
35. Gupta A, Antonsen T M (Jr.), Milchberg H M *Phys. Rev. E* **70** 046410 (2004)
36. Kim K Y et al. *Phys. Rev. Lett.* **90** 023401 (2003)

37. Petrov G M et al. *Phys. Rev. E* **71** 036411 (2005)
38. Kim H-Y et al. *Phys. Rev. A* **72** 053201 (2005)
39. Jungreuthmayer C et al. *Phys. Rev. Lett.* **92** 133401 (2004)
40. Fukuda Y et al. *Phys. Rev. A* **73** 031201(R) (2006)
41. Gavrilenko V P et al. *Phys. Rev. A* **73** 013203 (2006)
42. Sakabe S et al. *Phys. Rev. A* **74** 043205 (2006)
43. Last I, Jortner J *Phys. Rev. A* **60** 2215 (1999)
44. Martchenko T et al. *Phys. Rev. A* **72** 053202 (2005)
45. Micheau S et al. *J. Phys. B: At. Mol. Opt. Phys.* **38** 3405 (2005)
46. Gets A V, Krainov V P *J. Phys. B: At. Mol. Opt. Phys.* **39** 1787 (2006)
47. Bornath Th, Hilse P, Schlanges M *Laser Phys.* **17** 591 (2007)
48. Fukuda Y, in *Topical Problems of Nonlinear Wave Physics* (*NWP-2005*), *Proc. of Intern. Symp., St.-Petersburg – Nizhny Novgorod, Russia, August 2 – 9, 2005* (Proc. SPIE, Vol. 5975, Ed. A M Sergeev) (Bellingham, Wash.: SPIE, 2006)
49. Kundu M, Bauer D *Phys. Rev. A* **74** 063202 (2006)
50. Bauer D, Mulser P *Phys. Plasmas* **14** 023301 (2007)
51. Kidun O, Bauer D *J. Phys. B: At. Mol. Opt. Phys.* **40** 779 (2007)
52. Bauer D *J. Phys. B: At. Mol. Opt. Phys.* **37** 3085 (2004)
53. Ramunno L, Jungreuthmayer C, Brabec T *Laser Phys.* **17** 618 (2007)
54. Jungreuthmayer C et al. *J. Phys. B: At. Mol. Opt. Phys.* **38** 3029 (2005)
55. Ditmire T et al. *Phys. Rev. Lett.* **75** 3122 (1995)
56. Ditmire T et al. *Appl. Phys. Lett.* **71** 166 (1997)
57. Smirnov M B *Zh. Eksp. Teor. Fiz.* **124** 48 (2003) [*JETP* **97** 42 (2003)]
58. Smirnov M B *Phys. Scripta* **107** 149 (2004)
59. Ditmire T et al. *Phys. Rev. Lett.* **78** 3121 (1997)
60. Lei A et al. *Chinese Phys.* **9** 432 (2000)
61. Borisov A B et al. *J. Phys. B: At. Mol. Opt. Phys.* **29** L113 (1996)
62. Parra E et al. *Phys. Rev. E* **62** R5931 (2000)
63. Adoui L et al. *Nucl. Instrum. Meth. B* **205** 341 (2003)
64. Kubiak G D et al. *OSA Trends Opt. Photon. Ser. Extreme Ultraviolet Lithogr.* **4** 66 (1996)
65. Zweiback J et al. *Phys. Rev. Lett.* **84** 2634 (2000)
66. Zweiback J et al. *Phys. Rev. Lett.* **85** 3640 (2000)
67. Grillon G et al. *Phys. Rev. Lett.* **89** 065005 (2002)
68. Madison K W et al. *Phys. Plasmas* **11** 270 (2004)
69. Symes D R et al. *Chinese Phys. Lett.* **23** 2956 (2006)
70. Sakabe S et al. *Phys. Rev. A* **69** 023203 (2004)
71. Liu C S, Tripathi V K *Phys. Plasmas* **10** 4085 (2003)
72. Fukuda Y et al. *Phys. Rev. A* **67** 061201 (2003)
73. Issac R C et al. *Phys. Plasmas* **11** 3491 (2004)
74. Hansen S B et al. *Phys. Rev. E* **71** 016408 (2005)
75. Zharova N A, Litvak A G, Mironov V A *Zh. Eksp. Teor. Fiz.* **128** 844 (2005) [*JETP* **101** 728 (2005)]
76. Milchberg H M, McNaught S J, Parra E *Phys. Rev. E* **64** 056402 (2001)
77. Kim K Y et al. *Phys. Plasmas* **11** 2882 (2004)
78. Kim K Y et al. *Phys. Rev. A* **71** 011201(R) (2005)
79. Dobosz S et al. *Pis'ma Zh. Eksp. Teor. Fiz.* **68** 454 (1998) [*JETP Lett.* **68** 485 (1998)]
80. Larsson J, Sjögren A *Rev. Sci. Instrum.* **70** 2253 (1999)
81. Dobosz S et al. *Zh. Eksp. Teor. Fiz.* **115** 2051 (1999) [*JETP* **88** 1122 (1999)]
82. Honda H et al. *Phys. Rev. A* **61** 023201 (2000)
83. Auguste T et al. *Pis'ma Zh. Eksp. Teor. Fiz.* **72** 54 (2000) [*JETP Lett.* **72** 38 (2000)]
84. Mocek T et al. *Appl. Phys. Lett.* **76** 1819 (2000)
85. Ter-Avetisyan S et al. *J. Appl. Phys.* **94** 5489 (2003)
86. Mocek T et al. *Phys. Rev. E* **62** 4461 (2000)
87. Abdallah J (Jr.) et al. *Phys. Rev. A* **63** 032706 (2001)
88. Abdallah J (Jr.) et al. *Phys. Rev. A* **68** 063201 (2003)
89. Rozet J P *Phys. Scripta* **92** 113 (2001)
90. Sobelman I I *Atomic Spectra and Radiative Transitions* (Berlin: Springer-Verlag, 1979)
91. Lisitsa V S *Atoms in Plasmas* (Berlin: Springer-Verlag, 1994)
92. Pal'chikov V G, Shevelko V P *Reference Data on Multicharged Ions* (Berlin: Springer-Verlag, 1995)
93. Zatsarinny O et al. *Astron. Astrophys.* **426** 699 (2004)
94. Sobelman I I, Vainshtein L A, Yukov E A *Excitation of Atoms and Broadening of Spectral Lines* (Berlin: Springer-Verlag, 1981)
95. Junkel-Vives G C et al. *Phys. Rev. E* **65** 036410 (2002)
96. Last I, Jortner J *J. Phys. Chem. A* **106** 10877 (2002)
97. Flambaum V V et al. *Phys. Rev. A* **66** 012713 (2002)
98. Vaeck N, Kylstra N J *Phys. Rev. A* **65** 062502 (2002)
99. Brody T A et al. *Rev. Mod. Phys.* **53** 385 (1981)
100. Deiss C et al. *Phys. Rev. Lett.* **96** 013203 (2006)
101. Peano F, Fonseca R A, Silva L O *Phys. Rev. Lett.* **94** 033401 (2005)
102. Hohenberger M et al. *Phys. Rev. Lett.* **95** 195003 (2005)
103. Dorchies F et al. *Phys. Rev. E* **71** 066410 (2005)
104. Li H et al. *Phys. Rev. A* **74** 023201 (2006)
105. Mijoule V, Lewis L J, Meunier M *Phys. Rev. A* **73** 033203 (2006)
106. Isla M, Alonso J A *Phys. Rev. A* **72** 023201 (2005)
107. Krainov V P, Smirnov B M *Zh. Eksp. Teor. Fiz.* **132** 634 (2007) [*JETP* **105** 559 (2007)]
108. Siedschlag C, Rost J M *Phys. Rev. A* **67** 013404 (2003)
109. Li S H *Acta Phys. Sinica* **54** 636 (2005)
110. Kumarappan V, Krishnamurthy M, Mathur D *Phys. Rev. A* **67** 043204 (2003)
111. Kostenko O F, Andreev N E *Fiz. Plazmy* **33** 556 (2007) [*Plasma Phys. Rep.* **33** 503 (2007)]
112. Islam M R, Saalmann U, Rost J M *Phys. Rev. A* **73** 041201(R) (2006)
113. Jha J, Mathur D, Krishnamurthy M *J. Phys. B: At. Mol. Opt. Phys.* **38** L291 (2005)
114. Chen G et al. *J. Phys. B: At. Mol. Opt. Phys.* **40** 445 (2007)
115. Schmidt R, Seifert G, Lutz H O *Phys. Lett. A* **158** 231 (1991)
116. Seifert G, Schmidt R, Lutz H O *Phys. Lett. A* **158** 237 (1991)
117. Basbas G, Ritchie R H *Phys. Rev. A* **25** 1943 (1982)
118. Eliezer S, Martinez-Val J M, Deutsch C *Laser Part. Beams* **13** 43 (1995)
119. Bret A, Deutsch C *Fusion Eng. Design* **32 – 33** 517 (1996)
120. Deutsch C et al. *Fusion Technol.* **3** (1) 1 (1997)
121. Zwicknagel G, Deutsch C *Phys. Rev. E* **56** 970 (1997)
122. Bret A, Deutsch C *Nucl. Instrum. Meth. A* **415** 703 (1998)
123. Becker E W, Bier K, Henkes W *Z. Phys.* **146** 333 (1956)
124. Henkes W *Z. Naturforsch. A* **16** 842 (1961)
125. Henkes W *Z. Naturforsch. A* **17** 786 (1962)
126. Hagena O F, Obert W *J. Chem. Phys.* **56** 1793 (1972)
127. Hagena O F *Surf. Sci.* **106** 101 (1981)
128. Hagena O F *Z. Phys. D* **4** 291 (1987); **17** 157 (1990); **20** 425 (1991)
129. Takagi T *Ionized-Cluster Beam Deposition and Epitaxy* (Park Ridge, NJ: Noyes Publ., 1988)
130. Aleksandrov M L, Kusner Yu S *Gazodinamicheskie Molekulyarnye, Ionnye i Klasternye Puchki* (Gasdynamic Molecular, Ion, and Cluster Beams) (Leningrad: Nauka, 1989)
131. Haberland H (Ed.) *Clusters of Atoms and Molecules*: *Theory, Experiment, and Clusters of Atoms* (Springer Series in Chemical Physics, Vol. 52) (Berlin: Springer-Verlag, 1995)
132. Smirnov B M *Usp. Fiz. Nauk* **167** 1169 (1997) [*Phys. Usp.* **40** 1117 (1997)]
133. Smirnov B M *Usp. Fiz. Nauk* **170** 495 (2000) [*Phys. Usp.* **43** 453 (2000)]
134. Smirnov B M *Usp. Fiz. Nauk* **173** 609 (2003) [*Phys. Usp.* **46** 589 (2003)]
135. Smirnov B M *Contrib. Plasma Phys.* **44** 558 (2004)
136. Smirnov B M, in *Entsiklopediya Nizkotemperaturnoi Plazmy* (Encyclopedia of Low-Temperature Plasma) Vol. 8 (Ed.-in-Chief V E Fortov) (Moscow: Yanus-K, 2006)
137. Parks P B et al. *Phys. Rev. A* **63** 063203 (2001)
138. Kishimoto Y, Masaki T, Tajima T *Phys. Plasmas* **9** 589 (2002)
139. Smirnov B M *Pis'ma Zh. Eksp. Teor. Fiz.* **81** 8 (2005) [*JETP Lett.* **81** 6 (2005)]
140. Fermi E, Teller E *Phys. Rev.* **72** 399 (1947)
141. Smirnov B M *Zh. Eksp. Teor. Fiz.* **44** 192 (1963) [*Sov. Phys. JETP* **17** 133 (1963)]
142. Lifshitz E M, Pitaevskii L P *Fizicheskaya Kinetika* (Physical Kinetics) (Moscow: Nauka, 1979) [Translated into English (Oxford: Pergamon Press, 1981)]

143. Landau L D, Lifshitz E M *Kvantovaya Mekhanika*: *Nerelyativistskaya Teoriya* (Quantum Mechanics: Non-Relativistic Theory) (Moscow: Nauka, 1974) [Translated into English (Oxford: Pergamon Press, 1980)]
144. Bosch H-S, Hale G M *Nucl. Fusion* **32** 611 (1992)
145. Krainov V P, Smirnov B M, in *Ekstremal'noe Sostoyanie Veshchestva* (Extreme States of Substances) (Eds V E Fortov et al.) (Chernogolovka: IPKhF RAN, 2006)
146. Smirnov B M *Physics of Ionized Gases* (New York: John Wiley, 2001)
147. Ditmire T et al. *Nature* **398** 489 (1999)
148. Ditmire T et al. *Phys. Plasmas* **7** 1993 (2000)
149. Hilscher D et al. *Phys. Rev. E* **64** 016414 (2001)
150. Madison K W et al. *J. Opt. Soc. Am. B* **20** 113 (2003)
151. Ter-Avetisyan S et al. *Phys. Plasmas* **12** 012702 (2005)
152. Norreys P A et al. *Plasma Phys. Control. Fusion* **40** 175 (1998)
153. Disdier L et al. *Phys. Rev. Lett.* **82** 1454 (1999)
154. Madison K W et al. *Phys. Rev. A* **70** 053201 (2004)
155. Buersgens F et al. *Phys. Rev. E* **74** 016403 (2006)
156. Symes D R et al. *Phys. Rev. Lett.* **98** 123401 (2007)
157. Liu H J et al. *Chinese Phys. Lett.* **24** 494 (2007)
158. Schnürer M et al. *Phys. Rev. E* **70** 056401 (2004)
159. Ter-Avetisyan S et al. *Phys. Rev. Lett.* **93** 155006 (2004)
160. Karsch S et al. *Phys. Rev. Lett.* **91** 015001 (2003)
161. Last I, Jortner J *Phys. Rev. Lett.* **97** 173401 (2006)
162. Last I, Jortner J *Phys. Rev. A* **73** 013202 (2006)
163. Ter-Avetisyan S et al. *Phys. Rev. Lett.* **96** 145006 (2006)
164. Emsley J *The Elements* 2nd ed. (Oxford: Clarendon Press, 1991)
165. Mesyats G A, Yalandin M I *Usp. Fiz. Nauk* **175** 225 (2005) [*Phys. Usp.* **48** 211 (2005)]
166. Hagena O F *Rev. Sci. Instrum.* **63** 2374 (1992)